

ScholarWorks@GSU

Authigenic Minerals: Locality 80, Bed I Tuffs, Olduvai Gorge, Tanzania

Authors	Jarrett, Robert E.
Citation	Jarrett, Robert E. Authigenic Minerals: Locality 80, Bed I Tuffs, Olduvai Gorge, Tanzania. May 2014, Georgia State University. https://doi.org/10.57709/5530436 .
DOI	https://doi.org/10.57709/5530436
Download date	2026-04-11 03:09:47
Link to Item	https://hdl.handle.net/20.500.14694/6457

5-10-2014

Authigenic Minerals: Locality 80, Bed I Tuffs, Olduvai Gorge, Tanzania

Robert E. Jarrett
Georgia State University

Follow this and additional works at: http://scholarworks.gsu.edu/geosciences_theses

Recommended Citation

Jarrett, Robert E., "Authigenic Minerals: Locality 80, Bed I Tuffs, Olduvai Gorge, Tanzania." Thesis, Georgia State University, 2014.
http://scholarworks.gsu.edu/geosciences_theses/74

This Thesis is brought to you for free and open access by the Department of Geosciences at ScholarWorks @ Georgia State University. It has been accepted for inclusion in Geosciences Theses by an authorized administrator of ScholarWorks @ Georgia State University. For more information, please contact scholarworks@gsu.edu.

AUTHIGENIC MINERALS: LOCALITY 80, BED I TUFFS,
OLDUVAI GORGE, TANZANIA

by

ROBERT E. JARRETT

Under the Direction of Daniel M. Deocampo

ABSTRACT

Understanding climatic and water-mineral chemistry affecting hominin habitats during the period 1.92 to 1.80 Ma in Paleolake Olduvai basin, Tanzania is of social and scientific interest. Previous Olduvai research reported climate cycles in bulk sample mineral analyses. X-ray diffraction, X-ray fluorescence, and color analyses of Locality 80 Tuff Bed I samples tested the null hypothesis: Alteration mineralogy of Central Basin volcanic Tuffs IA through IF reflect salinity/alkalinity cycles. Such cyclicity was not found. Several primary authigenic minerals were confirmed, but not as previously reported. Tuffs are thoroughly altered, mostly to potassium-feldspars, zeolites, and carbonates, plus other feldspars and clay minerals (clays not in this study). Nevertheless, other findings reveal there is more to be learned. Results imply a major geochemical shift around 1.869-1.857 Ma, from non-zeolite forming environments to zeolite forming environments. A newly developed age model could aid re-analysis of past work and assist future research.

INDEX WORDS: Age model, Authigenesis, Bed I, Climate cycle, Paleolake Olduvai, Phillipsite, Tuff alteration, Zeolite

AUTHIGENIC MINERALS: LOCALITY 80, BED I TUFFS,
OLDUVAI GORGE, TANZANIA

by

ROBERT E. JARRETT

A Thesis Submitted in Partial Fulfillment of the Requirements for the Degree of

Master of Science

in the College of Arts and Sciences

Georgia State University

2014

Copyright by
Robert E Jarrett
2014

AUTHIGENIC MINERALS: LOCALITY 80, BED I TUFFS, OLDUVAI GORGE,
TANZANIA

by

ROBERT E. JARRETT

Committee Chair: Daniel Michael Deocampo

Committee: W. Crawford Elliott
Lawrence M. Kiage

Electronic Version Approved:

Office of Graduate Studies
College of Arts and Sciences
Georgia State University
May 20, 2014

DEDICATION

To Olga, who, as co-geo-enthusiast, got me into this and helped me get out.

ACKNOWLEDGEMENTS

Dr. Daniel. M. Deocampo, committee chair, my enthusiastic, patient, and knowledgeable advisor and often amused bystander

Dr. W. Crawford Elliott, committee member, who helped me get into the program and provided valued intellectual stimulation and knowledge these too many years

Dr. Lawrence Kiage, committee member, who courageously said “yes” without hesitation and got me successfully started through a software thicket

Ms. Patricia Berry, project predecessor and initial information provider

Dr. Gail M. Ashley, author of many valuable articles, mentor to many on the road to full understanding of Olduvai Gorge, and kind source of advice and information

Dr. Alan Deino, whose research and willing counsel freed me from a blind corner

Ms. Rebecca Pickering and Ms. Lucy Taylor, fellow students, for numerous timely assists

Ms. Basirat Lawal, Ms. Tia Williams, and Ms. Quen'Naldria Drake, administrative staff, who catered to many needs

Dr. Jeremy E. Diem, the graduate director, tugging and hauling to get us all done on time

TABLE OF CONTENTS

ACKNOWLEDGEMENTS	v
LIST OF TABLES	x
LIST OF FIGURES	xi
ABBREVIATIONS	xii
1 INTRODUCTION	1
1.1 Significance	1
1.2 Purpose	1
1.3 Expected Results	1
1.4 Location	2
1.5 Physical Setting	3
1.6 Geology, Climate, and Hydrology	4
1.6.1 General	4
1.6.2 Geology	5
1.6.3 Climate	10
1.6.4 Hydrology	14
1.6.4.1 Surface Water	14
1.6.4.2 Groundwater	15
1.6.5 Authigenesis	16
1.6.6 Age Research and Modeling	21
2 METHODS	22
2.1 Samples	22
2.2 Age Model	24

2.2.1	<i>Preliminary Remarks</i>	24
2.2.2	<i>Age Model Detailed discussion</i>	25
2.3	Analytical Methods	28
2.3.1	<i>X-ray Diffraction (XRD)</i>	28
2.3.2	<i>Re-analysis of X-ray fluorescence (XRF)</i>	30
2.3.3	<i>Munsell Color Comparison</i>	31
2.3.4	<i>Statistical Analysis</i>	31
3	RESULTS	32
3.1	Age Model Reconciliation	32
3.2	Tuff Mineralogy	33
3.2.1	<i>X-ray Diffraction</i>	33
3.2.2	<i>Re-analysis of X-ray fluorescence (XRF)</i>	33
3.2.3	<i>Combined Findings of XRD and XRF Analyses</i>	40
3.2.4	<i>Tuff Color</i>	42
3.2.5	<i>Statistical Analyses</i>	43
4	DISCUSSION	45
4.1	Age Model	45
4.2	Tuff Mineralogy	46
4.2.1	<i>X-ray Diffraction (XRD)</i>	46
4.2.2	<i>Combined Findings of XRD and XRF Analyses - Cyclic Relationship</i>	47
4.2.3	<i>Authigenesis</i>	48
4.2.3.1	Authigenic Phillipsite and Sanidine Climate Cycle Proxies	48
4.2.3.2	Ammonium Phillipsite	49

4.2.3.3	Suite of Zeolites	50
4.2.4	<i>Cation Oxide Comparisons</i>	50
4.2.5	<i>Tuff Color Analysis</i>	52
4.2.6	<i>Unanticipated Findings</i>	52
4.2.6.1	1.869-1.857 Ma Authigenesis Transition	52
4.2.6.2	Potential Micro-cycles	53
4.2.6.3	Groundwater	53
4.3	Paleo-environmental Implications	54
4.4	Future Work	55
5	CONCLUSIONS	56
5.1	Age Model	56
5.2	Mineralogy	57
5.3	1.869-1.857 Ma Authigenesis	57
	REFERENCES	59
	APPENDICES	63
	Appendix A: Berry (2012) XRF oxide data for Bed I Tuffs	63
	Appendix B: Minerals cited in Olduvai Gorge literature	65
	Appendix C: Age Model Development	67
	<i>Appendix C.1: Age Model: Summarized Results</i>	67
	<i>Appendix C.2: Basic Stratichronology Ages</i>	68
	<i>Appendix C.3: Deposit Age Reconciliation Computations</i>	69
	<i>Appendix C.4: Sample Depth - Age Conversion Chart</i>	73
	Appendix D: XRD-determined Major Authigenic Minerals: Tuffs IA - IF	74

Appendix E: Tuff Deposition History	75
Appendix F: Variations on Alkali Oxide Ratios vs. Ca/MgO	76
Appendix G: All Tuff Oxide Data for TriPlot - 25 Tuffs	77
Appendix H: Major Cations in Zeolites and Primary & Secondary Non-Zeolites	78
Appendix I: Tuff Age & Tuff Type vs. CaO/MgO Ratio	79
Appendix J: Tuff Age & Tuff Type vs. Al₂O₃/MgO Ratio	80
Appendix K. Cation Oxide Statistical Analysis	81
<i>Appendix K.1 Variable Input Data</i>	<i>81</i>
<i>Appendix K.2 Correlation Contingency Table</i>	<i>81</i>
Appendix L: XRD Diffraction Scans	82

LIST OF TABLES

Table 1 Comparison of wet and dry peak research	10
Table 2 Bed I tuff ages and sedimentation rate multipliers	25
Table 3 Required stratigraphic data adjustments	26
Table 4 Possible intra-Bed I discontinuities	27
Table 5 Tabular age model and summary XRD output	34
Table 6 Munsell soil color Analysis	43

LIST OF FIGURES

Figure 1 Continental and regional location	2
Figure 2 Local feature relationships	3
Figure 3 Loc 80 stratigraphic column and lithology of selected constituents	6
Figure 4 Schematic of Bed I on completion of Tuff IF at 1.803 Ma	7
Figure 5 Generalized map of the Olduvai Gorge locale	9
Figure 6 Olduvai and Ngorongoro area map	9
Figure 7 Paleolake Olduvai cycles: Five complete lake cycles are represented	13
Figure 8 Schematic cross-section showing presumed overall water flow	15
Figure 9 Locality 80 sampling trench	23
Figure 10 XRD system with the sample loading on the reflection transmission spinner	29
Figure 11 Sample diffraction scan: Locality 80 Tuff ID sample GA-L-61-99, 1.839 Ma	30
Figure 12 Tuff deposition history related to Berry (2012) wet and dry cycles	36
Figure 13 Tuff (Na ₂ O +K ₂ O) vs. CaO/MgO ratios: Phillipsite vs. non-phillipsite regimes	37
Figure 14 Tuff (Na ₂ O + K ₂ O)%/MgO% vs. CaO%/MgO%	38
Figure 15 Triangular plot of tuff oxides	39
Figure 16 Major cations in zeolites and primary and secondary non-zeolite minerals	40
Figure 17 Tuff age & tuff type vs. CaO/MgO ratio	41
Figure 18 Tuff age & tuff types vs. Al ₂ O ₃ /MgO wt.% ratio	42

LIST OF ABBREVIATIONS

AFM	Triangular diagram based on Na ₂ O + K ₂ O, FeO, and MgO content
Al	Aluminum
Al ₂ O ₃	Aluminum Oxide
amsl	Above mean sea level
⁴⁰ Ar/ ³⁹ Ar	Ratio of Argon 40 / Argon 39 isotopes
Avg.	Average
Ca	Calcium
CaO	Calcium oxide
CB	Central Basin
__-CO ₃	The designated carbonate
δD	Ratio comparing deuterium content in hydrogen-isotope containing substances
Eh	Oxidation-reduction potential (volts)
<i>F</i>	Degrees of freedom in statistical analysis
K	Potassium
K ₂ O	Potassium Oxide
K-spar	Potassium feldspar
Ky	Thousand years
Loc 80	Locality 80
Ma	Million years ago
Mg	Magnesium
MgO	Magnesium Oxide
Na	Sodium
Na ₂ O	Sodium Oxide
<i>p</i>	Probability that a case falls outside the null hypothesis that populations are the same
pH	-log ₁₀ (H ⁺)
<i>r or R</i>	Correlation coefficient
<i>r² or R²</i>	<i>Coefficient of determination</i> , r-squared; proportion of variance that is explained
SPSS	Actual name of a specific proprietary statistical program
T	Temperature
XRD	X-Ray diffraction
XRF	X-Ray fluorescence

1. INTRODUCTION

1.1 Significance

Since Kattwinkel's 1911 discovery of extinct mammal fossils at the then newly found Olduvai Gorge, Tanzania, further explored by Reck in 1913 while on a geological investigation, and Leakey's recognition of artifacts among those bones in 1928, the search for and research on *genus Homo* (hominins) began there and continues today (Hay, 1976; Dawson, 2008). Leakey started onsite anthropological digs and analyses in 1931.

Interdisciplinary research in anthropology, archaeology, biology, climatology, geology, limnology, and paleontology aims to trace the path of pre-human evolution at that site, through studies of fossils, artifacts, life traces, faunal/floral variations, and age and climate indicators. Olduvai Gorge is thus far one of the few places the human race might identify as its site of origin on the way to becoming human then "modern". Time and climate are critical variables for these investigations. Their definition is central to success in all facets. This study is focused on conditions at and history of Bed I at Locality 80 (Loc 80).

1.2 Purpose

This work investigates the mineralogy of tuff deposits in Bed I. These data may be used to test, in part, the hypothesis that climate cycles during the formation of Bed I sediments can be discerned and exactly placed in time. They could then be used as proxies for surface water quality and livability of the local environment.

1.3 Expected Results

Based on prior researchers' work described later, the hypothesis is: X-ray diffraction analysis of the tuffs will confirm that lakebed sediment mineralogies can be correlated to cycles of highly saline / alkaline waters in driest-climate, relatively smaller, paleolake Olduvai

environments (and will be temporally distinctive) when compared to cycles of wettest-climate, relatively larger, less concentrated paleolake Olduvai environments. That is, results will show the same cyclicity found by other work and perhaps sharpen cycle duration and / or intensity estimates leading to identification of causes or explanations for this cyclicity.

1.4 Location

Olduvai Gorge is part of the Ngorongoro Conservation Area, Ngorongoro Division, of Arusha Region in the northeastern corner of Tanzania. The main and side gorge floors of Olduvai Gorge, Tanzania meet at coordinates $35^{\circ} 21.193'E$ and $2^{\circ} 59.459'S$, elevation 1411 m amsl (Google Earth, 2014).

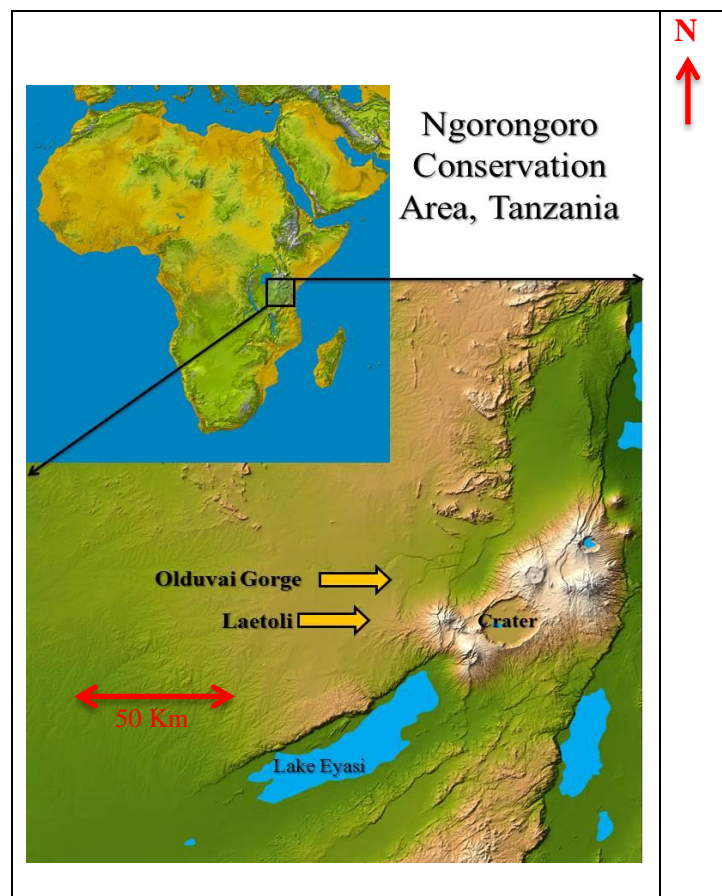


Figure 1 Continental and regional location (The Laetoli-Olduvai Field School, 2014)

The approximate center of fossil hominin finds is at the juncture of seasonal streams in the Main and Side Gorges (yellow circle on Figure 2), which is about 30 Km northwest of the center of Ngorongoro volcanic crater.

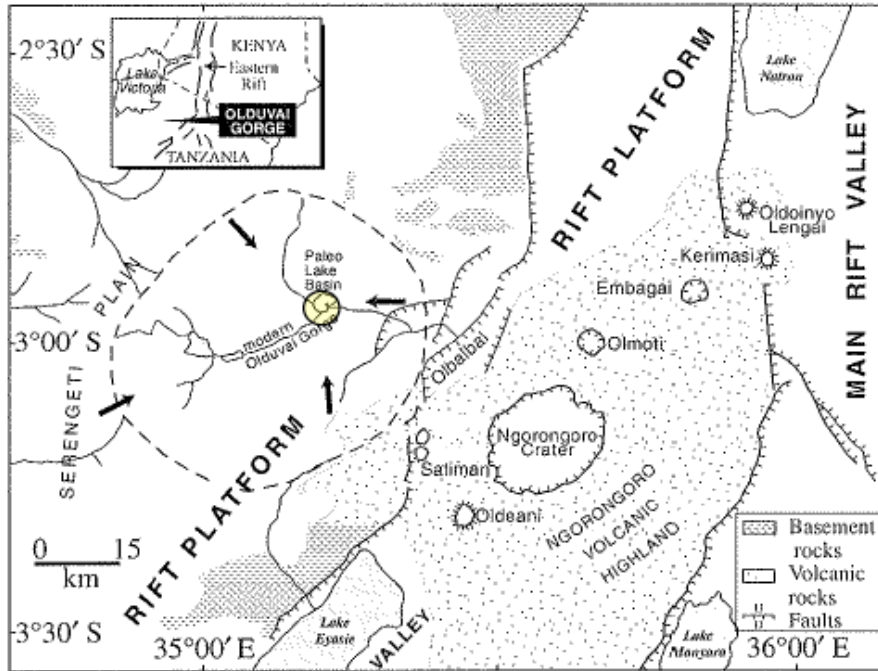


Figure 2 Local feature relationships
 Pleistocene sedimentary rocks constitute the bulk of uncoded land surfaces (After Berry, 2012; after Ashley, 2007; after Hay, R.L. and Kyser T.K., 2001)

1.5 Physical Setting

The Gorge is incised approximately 100 m into the eastern side of Serengeti Plain with large, extinct volcanoes to the southeast and east and active Oldoinyo Lengai to the east-northeast. Locality 80, source of samples for this study, is on the north side of the Main Gorge at approximately 35° 18.664'E and 2° 57.793'S and slightly northwest of the stream juncture (Hay, 1976; Ashley et al., 1999; Google Earth, 2014). Regional drainage is from the west and east toward the Olbalbal depression, a fault graben-formed depression primarily composed of volcanic alluvial deposits with an ephemeral lake / wetland. Olbalbal is a modern surface and groundwater runoff sump for Olduvai Gorge and for the nearby volcanic areas (Hay, 1976). This

ephemeral wetland serves the same regional closed-basin purpose to collect and concentrate surface and groundwater and their dissolved salts as Paleolake Olduvai once did, although it is much smaller. The Gorge formed from 400 Ka (Hay, 1976) until 50-30 Ka (Leakey et al., 1972; Sinclair et al., 2009; Zimmermann, 2013). Paleolake Olduvai drained, as the result of erosion promoted by the progressive subsidence of a series of grabens to the east. Hay (1976) wrote that tectonic activity lowered Lake Olduvai to the east beginning at or near the end of Bed II deposition. Stollhofen and Stanistreet (2012) concluded that most faults were active throughout the times of greatest deposition. They assert the lake (sump) had completely vacated the Central Basin (CB), the typically low-level closed-basin body size, by the start of the Masek period.

1.6 Geology, Climate, and Hydrology

1.6.1 General

From west to east, Olduvai Basin sedimentary deposits are neighbored and underlain by Precambrian metamorphic rocks, punctuated by inselbergs of metamorphic rocks, and bordered on the east by two million year old Pliocene-Pleistocene to Holocene volcanic deposits (Hay, 1976; Ashley et al., 2010b). These deposits include not only volcanic calderas but complex layering of ashes and lavas, alluvial materials from several sources, and, quite significantly, those materials after alteration by a wide range of mutually confounding physical, chemical, and biological processes. As seen in Figure 2, roughly parallel normal faults associated with rifting cross the area. The region's geologic and biological history has been strongly influenced by Gregory East Africa Rift Zone processes. It is a region of rift extension, graben faulting, and subsidence (Hay, 1976). As a result, groundwater composition and flow are likely to have been and still remain complex. Baker (1986) describes a roughly analogous rifting, graben-forming, closed basin creation process for the northern half of the Kenyan Rift Valley, which about 2 Ma

gave rise to an inner graben and hypersaline Lakes Natron and Magadi, as well as lesser lakes. In both regions, faults and grabens in concert with arid climates produced closed, sediment-filled basins where saline / alkaline lakes occurred.

1.6.2 Geology

Cenozoic crystalline metamorphic rocks comprise the basement, western neighboring watershed regions, and local outcrops. Pliocene-Pleistocene deposits up to 100 m thick fill a basin some 25 km in diameter (Hay, 1976). Those deposits include volcanic tuffs, detrital siliciclastics from the west, detrital volcanics carried by runoff from all directions, authigenic products of those materials, biotic residues, and fossils.

Collapse of Ngorongoro volcano to form a caldera around 2 Ma essentially set the stage for the region today (Hay 1976), having covered the future lake's basin bottom of crystalline rock with the Naabi ignimbrite upon which alluvium deposited. Then began the deposition and authigenesis of major successions; i.e., Beds I, II, III, IV, Masek, Nduu, Naisiusiu, and Namorod. These beds were named and criteria refined based on occurrence of volcanic "marker beds" that could be traced over most of the basin. Eruptions of at least Ngorongoro and Olmoti deposited eolian and pyroclastic tuffs into what is believed to have been a shallow lake during Bed I formation, the first of the eight beds. Important Bed I marker tuffs are IA, IB, IC, ID, IE, and IF. These and un-named tuffs appearing at Loc 80 are the combined focus of this study. Figure 3 by Hay and Kyser (2001), though addressing mineral content of claystones rather than tuffs, provides a succinct picture of the stacking of tuff and non-tuff beds at Loc 80 relevant to this work.

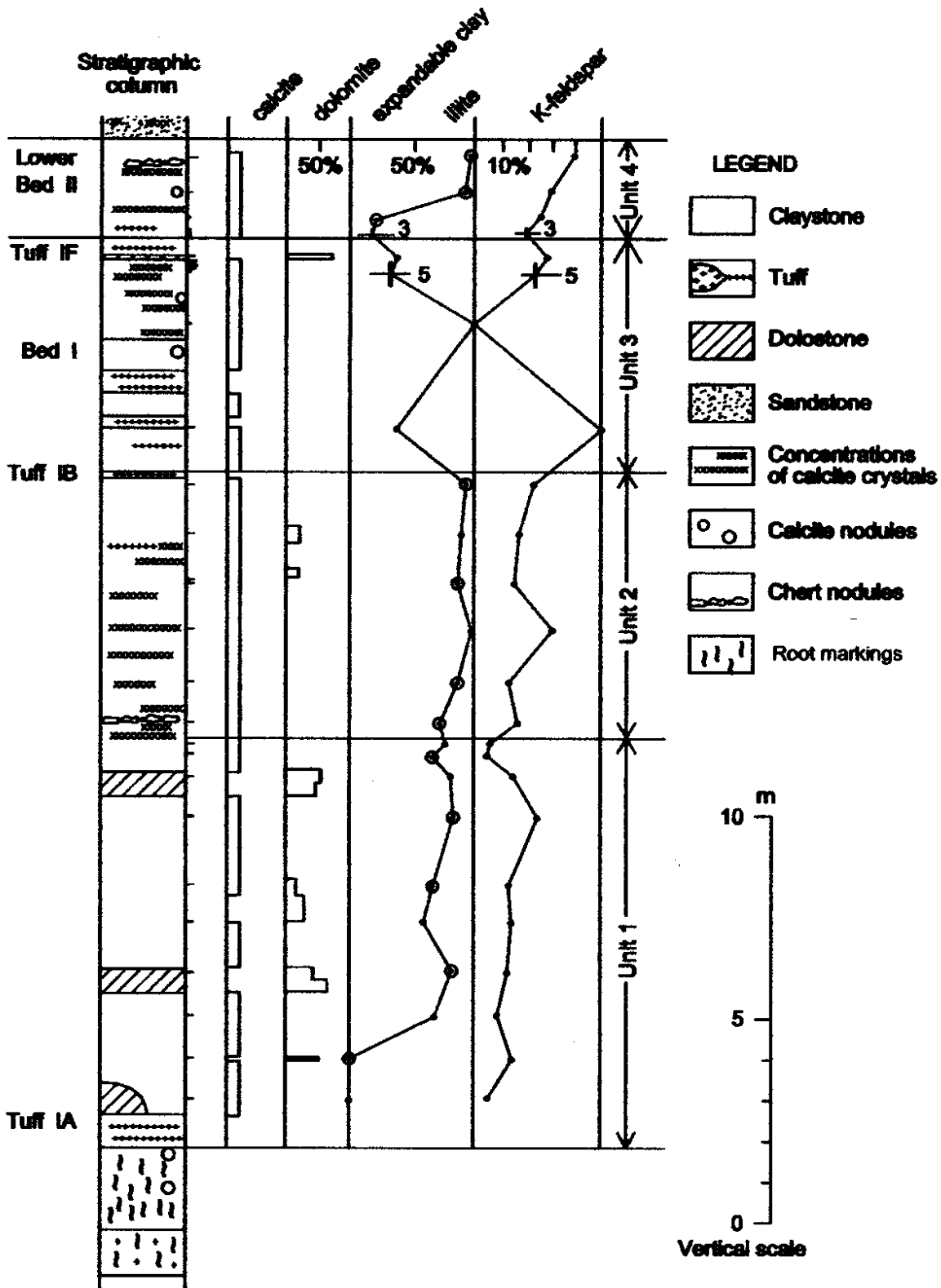


Figure 3 Loc 80 stratigraphic column and lithology of selected constituents
 Numbers above and below Tuff IF for "clay mineral" and "K-feldspar" are the n's for averages
 used by Hay and Kyser (2001) to plot their points.

The geological significance of Loc 80 derives from its: a) stratigraphic column completeness (all Beds I through Ndotu) and b) Bed I's almost complete coverage of the entire basin as a marker. Additionally, the oldest hominin fossils and artifacts (Oldowan culture) were found from just below Tuff IB to the top of Tuff IF at other locations in Olduvai Gorge (top of Bed I) (Hay, 1976). A critical attribute of Loc 80 was its location in the Central Basin (CB). Except for any periods of complete playa conditions the CB at Loc 80 was wet until the lake finally drained.

Hay goes on to describe Bed I as composed of these depositional environments: lacustrine, lake margin, alluvial fan, alluvial plain, and lava flow (Figure 4). The latter is found east of Paleolake Olduvai and is of no consequence to this study. These facies are interlayered. Their respective chemistries, together with evolving water quality conditions, apparently resulted in major authigenic changes in the original sediment mineral suites.

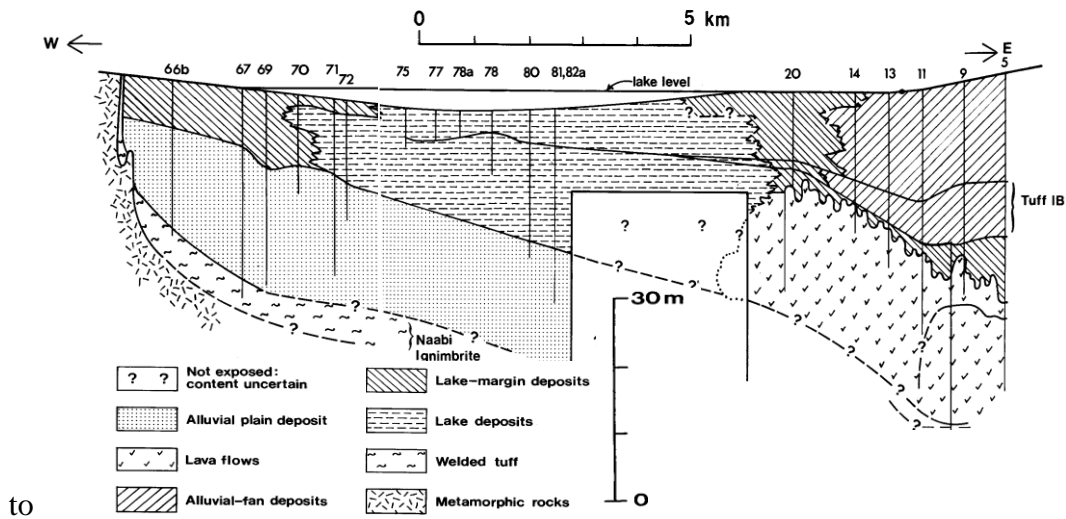


Figure 4 Schematic of Bed I on completion of Tuff IF at 1.803 Ma
Representation of Main Gorge North Side with sample site Locality 80 (after Hay, 1976)

Volcanic vents opened by tectonic extension periodically added ash and lava to the landscape. Tuff deposits were dispersed laterally over wide areas (Sikes and Ashley, 2007). Surface deposits (other than older crystalline outcrops) comprise Pliocene-Pleistocene-Holocene sequences of terrigenous eolian, volcanic-eolian, volcanic, fluvial, alluvial, and lacustrine sediments the older of which are lithified. Figures 5 and 6 below, though partially duplicative of preceding figures, include different elements. Figure 5 best portrays Paleolake Olduvai at high, mid, and lowstands, It likely was never more than a few meters deep, at its deepest. Gradual infilling of the basin would have contributed to lateral expansions recorded in the rock record. Olbalbal distal and proximal (to extinct volcanoes Lemagrut and Olmoti) alluvial fans, was a paleo-wetland near the Gorge junction, and ephemeral water courses. The distal fan hosts the ephemeral Lake Olbalbal depression. Figure 6 adds Locality 80 and a few other investigation sites, a box encompassing the highest interest anthropological sites, and key faults including Olbalbal fault (which hosts the current depression for water accumulation in a seasonal lake near the northeastern end of the alluvial fan) (Google Earth, 2014; Stollhofen & Stanistreet, 2012).

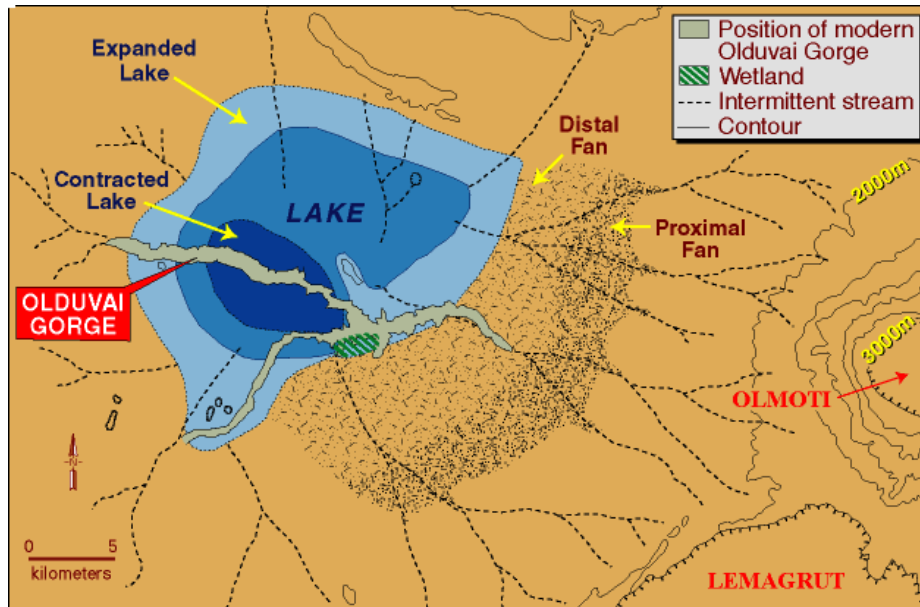


Figure 5 Generalized map of the Olduvai Gorge locale

Three hypothesized lake levels (dark blue = lowest; lightest blue = highest; likely never more than a few meters deep) and details of the Olbalbal distal and proximal alluvial fans receiving mountain and gorge runoff are seen. (Ashley et al. 2010a) "Contracted Lake" is used by some writers to signify the Central Basin (CB).

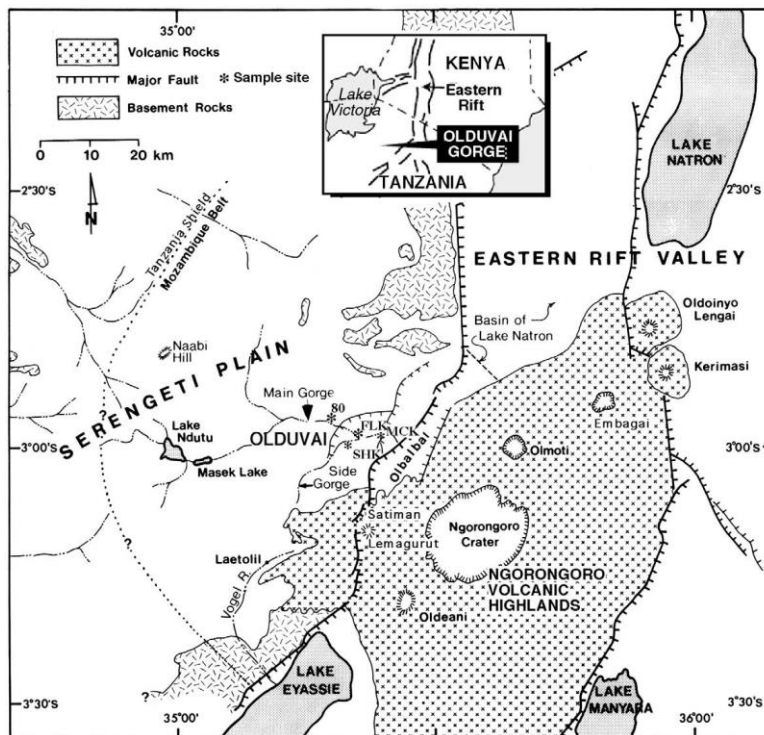


Figure 6 Olduvai and Ngorongoro area map

Loc 80 is left of the center and of the eastwardly dropping graben-faults (McHenry, 2009 after Hay, 1976)

1.6.3 Climate

Understanding climate in general, as a source of water, is crucial to understanding roles of authigenesis and its resulting mineral products on measured time scales. The authigenic minerals can often be used as proxies to estimate specific climatic and habitability conditions at given places and points in time. Ashley et al. (2010a) state there is consensus that climate drying occurred through the past 7 million years. That might be the general trend, but Potts (2013) pulls together the many facets of East African climate during the Plio-Pleistocene period of Olduvai Gorge history, including analysis of Earth orbital eccentricity, obliquity, and precession. He concludes that despite mathematical regularity and demonstrable inter-play of these Milankovitch cycles with other known climatic variables, there was much room for climatic variability, some of it abrupt. He identifies 1.89 to 1.69 Ma as one of the 200 ky high variability periods. It encompasses deposition of eight of this study's Bed I Tuffs GA-L-126-99 through IF. He goes on, saying that both aridity and high moisture times occurred during high variability periods.

Today the entire gorge and ancient lake area and semi-arid Serengeti Plain receive about 566 mm of rain per year (Cerling and Hay, 1986). Modern eastern highlands receive 1037 mm/yr (mean for 1987-1994) on the southwestern rim (Deocampo, 2004b). Ashley et al. (2010b) explain that with evaporation in the 2000-2500 mm/yr range, few permanent rivers and, by extension, lakes can exist in that region of Kenya and Tanzania. As can be seen from the maps, surface flows can arrive from the west and east, but their rain-fed ephemeral nature and high evaporation rates argue against high rates of fluvial sediment transport, except during infrequent flash flood conditions. They further explain that a large rain shadow of the Ngorongoro highlands reduces Olduvai Gorge rainfall much as it would have done when Beds I and II were

being laid down. Hay (1976) gives a height of 3000 m vs. 1360-1520 m for the Serengeti Plain. Ashley et al. (2014) cite Nicholson (1996) and Trauth et al. (2007) to the effect that today's easterly Indian Ocean weather patterns prevailed or were similar in Paleolake Olduvai times. That would mean paleo-conditions were similar to the following. Annual mean temperatures for one composite 12-month year drawn from 1972 and 1973 were minimum, 16.3°C and maximum, 29.3°C (Hay, 1976). The monthly low mean was July, 15.6°C with a monthly high mean in September at 30.7°C. This information suggests that temperatures would have been similar to those at many modern closed-basin lakes.

Deocampo (2004a) proposed the possibility of higher than Milankovitch frequencies in climate change. deMenocal (1995) studied eolian dust, biogenic opal, and organic carbon in marine sediments along with Earth precessional cycles to explore climate variability in Africa. Intervals of climate instability found by deMenocal around 2.8 and 1.7 Ma are both outside this study's focus of 1.920 to 1.800 Ma. In a time of general stability, orbitally and precessionally driven climate cycles should be easier to note than during the unstable preceding and succeeding periods. Stability is defined by fairly close adherence to Milankovitch cycles, as opposed to shorter-term responses to variables, such as "high latitude temperature changes".

Analysis of orbital cycles led Ashley (2007) (summarized with other's findings in Table1) to conclude that dry / wet peaks could have occurred in the latter half of this current study of Bed I. Ashley used an age model bounded by 1.845 Ma for Tuff IB (Blumenshine, 2003) and cited McHenry's (2005) 1.79 Ma for Tuff IF. Magill et al. (2013a) studied leaf lipid carbon and total carbon isotope ratios from lake margin sediments that suggested lake contractions and wet periods. They did not specifically state whether there was lake expansion or only a higher humidity climate. Working with Loc 80 leaf and algal lipid δD ratios, Magill et al. (2013b)

inferred a lake minimum and two maxima. They also inferred that ancient rainfall was in the 250-700 mm/yr range, as it currently is. It is unclear exactly what age model (in relation to Loc 80 depths) Magill et al. employed; therefore, unknown differences between models will prevent building a concordance of earlier findings and those of this study. The 1.79 Ma age for Tuff IF was revised backward with close tolerances to 1.803 +/- 0.002 Ma by Deino (2012), which raises questions about the ages in Table 1 based on Tuff IF being as young as 1.79 Ma. Results read from Berry (Figure 19, 2012) are included for comparison.

Table 1 Comparison of wet and dry peak research

Ashley (2007)		Magill et al. (2013a)		Magill et al. (2013b)		Berry (2012)	
Dry	Wet	Dry	Wet	Dry	Wet	Dry	Wet
						1.782	
1.79							
	1.80						1.801
1.81		1.807				1.812	
	1.82	1.820	1.819				1.820
1.83			1.831				
					1.835		
	1.84	1.840		1.843		1.839	
							1.847
			1.854		1.855		
						1.863	
							1.876
						1.907	

Berry (2012) reported higher resolution XRF-based geochemical interpretations of Bed I samples (clays and tuffs) deposited during times of both high salinity/alkalinity and relatively dilute conditions than did Hay and Kyser (2001), with agreement on most, but not all, occurrences of climatic wet-dry cycles. Berry's XRF data demonstrated five dry (lake contraction) and four wet (lake expansion) peaks (Appendix A and Figure 7).

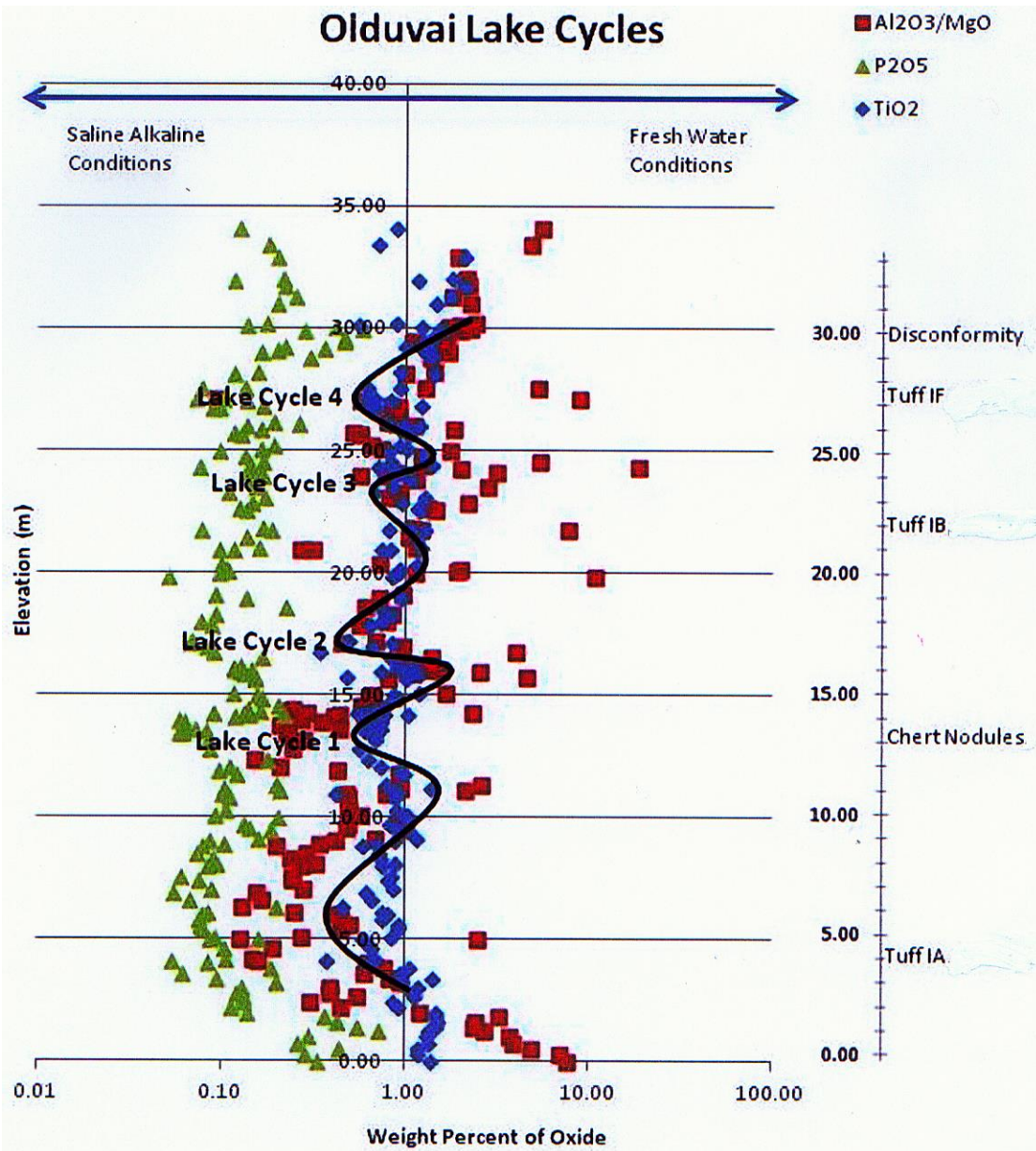


Figure 7 "Paleolake Olduvai cycles: Five complete lake cycles are represented Major oxide analysis demonstrates four major lake cycles. Each lake cycle begins and ends with a saline alkaline or dry phase. The Hay and Kyser (2001) sedimentation rates for age determination, 1 m = 5900 yr. for units 1 and 2 and 1 m = 8300 yr. for units 3 and 4, were used to determine the number of years required for each cycle to complete. Lake Cycle (LC) 1 completed in approximately 44,250 yrs, LC 2 completed in approximately 23,600 years, LC 3 completed in approximately 26,550 years and LC 4 completed in approximately 41,500 years. The average Lake Cycle is 33,975 years." (Berry, 2012) Peak highs and lows were visually extracted from data tables for each of the three oxide / oxide ratio variables, yielding 11 sets of three. Cluster %s by weight and elevations for each set were averaged, respectively, to make 11 elevation-Wt. % x-y pairs. EXCEL-generated the curve. (Berry, 2014)

In 1997, Bond et al. proposed, on the basis of marine core analyses, that the Holocene has experienced a series of 1470 +/- 500 yr. climate cycles in the North Atlantic. Gupta et al. (2003) further demonstrated evidence that southwestern Indian Ocean Monsoons responded to those climatic events.

1.6.4 Hydrology

1.6.4.1 Surface Water

As described in detail by Hay (1976) and since expanded upon by numerous researchers, including citations above, fluvial deposits, buried lateral fluvial channels, detrital sediment, surface topography, and discontinuities in CB deposits speak to a history of surface water additions to Paleolake Olduvai and erosion of its bed, when precipitation generated flowing water. "Rainy" periods would have seen occasional rapid level rises, but these rises would have been modest in the context of a constantly arid to semi-arid environment, as now seen for ephemeral Lake Olbalbal. Depending on conditions in the western, Precambrian uplands, there might or might not have been perennial stream flow at some times. If so, it was insufficient to keep CB levels high and waters dilute and overflowing out of the basin. Surface meteoric water contains low levels of chemical species dissolved from soils, rocks, biota (alive and dead), and the air that accumulate in hydraulically closed basins. The salts concentrate there from evaporation (Boggs, 2012). In any case, rainwater would have changed lake composition on both short and long temporal scales both by transport of salts to the basin and dilution of evaporatively concentrated water.

Referral to Figure 8 visually assists in grasping details of subsequent text on surface water and groundwater sources and movement.

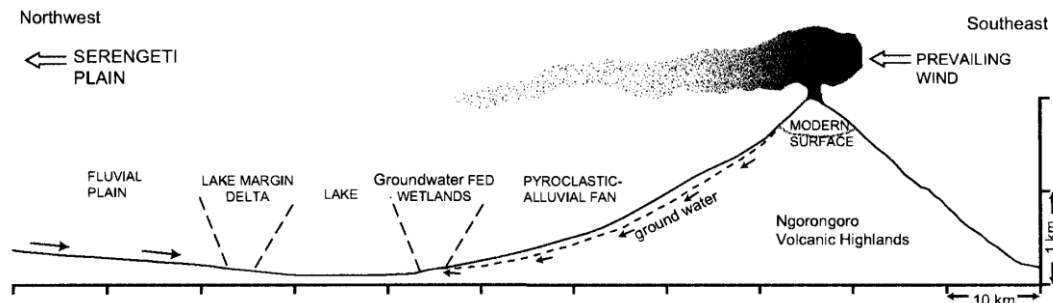


Figure 8 Schematic cross-section showing presumed overall water flow (Sikes and Ashley, 2007)

Earlier remarks spoke of tectonic lowering of the highly faulted eastern end of the basin through rifting, and the faults being active throughout sediment deposition (Stollhofen and Stanistreet, 2012). Key implications of the tilting would have been that western water had progressively easier access to the basin and that faults were and continued to be high permeability conduits (to be addressed under Groundwater). Eventually, the gorge developed and water flowed through to help form Lake Olbalbal in the then and now low-lying distal (from the volcanoes) alluvial fan.

1.6.4.2 Groundwater

Groundwater moves through volcanic cone deposits of the Ngorongoro highlands (3000 m) to emerge where faults, aquitards, aquicludes, and lowest depressions support springs and seeps (Deocampo, 2004b; Hay, 1976; Stollhofen and Stanistreet, 2012). Deocampo gives chemically verified Olmoti water contributions to Ngorongoro as evidence. Ashley et al. (2010b) describe finding spring tufa (carbonate deposits) physically associated with fossil hominin sites in upper Bed I. They cite similar geological and flow models delivering modern surface and subsurface Olmoti flows to the southeast and southwest to lakes Manyara and Eyasi where vegetation thrives (Ashley et al., 2010a). One might raise the objection that groundwater would have had to flow up-gradient westward to Lake Olduvai across uptilted graben block scarps. That objection might be valid were it not for the argument that the eastern subsidence and gorge

incision began (0.4 Ma) long after Bed I formed. Faults and permeable deposits could have delivered water westward to the lake margins and basin.

1.6.5 Authigenesis

Authigenesis is formation of minerals *in situ* by precipitation from water or after the protoliths' original placement (Bates and Jackson, 1984). It can also refer to direct precipitation from water. The search for authigenic, geochemical clues linked to climate and time are central elements for determining when and how hominins lived at Olduvai Gorge. How and when minerals currently found with fossils and artifacts formed inform reconstructions of habitat livability. In the Olduvai context, chemical authigenesis and differential precipitation could be mutually confounding in the record.

Eugster and Jones (1979) and Deocampo and Jones (2014) succinctly state mechanisms by which saline lakes (like modern Magadi and, by analogy, ancient Olduvai) evolve their characteristic solute suites. Evaporation causes concentration resulting in precipitation fractionation of solutes, sorption and exchange of active species like K^+ and SO_4^{-2} , and degassing: "The cationic evolution toward sodium dominance is caused mainly by precipitation of alkaline earth carbonates, gypsum, and Mg-silicates, whereas the anionic evolution away from bicarbonate dominance is related to precipitation of carbonates and sulfates coupled with degassing, sorption, and bacterial reduction of sulfates." They report Lake Magadi Na / K cation fractionating at as high a proportion as Na:K::1:100.

Bed I tuffs are no longer the pristine volcanic glasses and other minerals that originally fell into CB water (Deocampo, 2004a; Hay, 1976; Hay and Kyser, 2001; McHenry, 2009). Hay (1963) wrote:

Zeolites and dawsonite have formed rapidly during the past 20,000 years in the sides of Olduvai Gorge and over the adjacent Serengeti Plain of northeast

Tanganyika. Nephelinite tuffs were altered to form a surface calcrete and the minerals phillipsite, natrolite, chabazite, analcime, and dawsonite; sodic trachyte tuffs were altered to form phillipsite, erionite, and chabazite. Zeolites and calcrete were also formed at the land surface in the Olduvai region during two dry episodes of the Pleistocene before the gorge was eroded. Zeolites and dawsonite were formed by reaction of volcanic glass and nepheline with solutions of sodium carbonate and bicarbonate that were concentrated by evaporation in the soil and surface layers of rock. Hydration and carbonation appear to be the principal chemical changes in zeolitic alteration.

A key significance lies in the short time required for those reactions to happen to trachyte tuffs.

A large body of literature lists many authigenic minerals identified in Olduvai Bed I tuffs and conclusions that K-rich minerals and zeolites formed during dry climatic periods when Paleolake Olduvai Central Basin is believed to have become highly saline and alkaline. Larsen (2008) reported a literature consensus that zeolites (analcime, chabazite, and phillipsite among them) are common authigenic products of vitric tuff reactions with saline/alkaline waters, and that K-feldspars are common secondary authigenic products in similar environments with zeolites being the critical K source. Waters high in alkali element ions (especially K and Na) and in bicarbonate alkalinity react with volcanic glasses comprising tuffs to produce a range of minerals including structurally porous aluminosilicates (zeolites) and, or in turn, the other minerals listed in Appendix B, "Minerals cited". McHenry (2009) found phillipsite and chabazite "dominating" proximal lake margin sediments and phillipsite in the intermittently dry lake deposits. Regarding zeolite and K-spar authigeneses, Hay and Kyser (2001, their Figure 10) determined lake water salinity, when Tuff IA deposited, only modestly above geological average (slightly dilute, relatively speaking) from 1.924 Ma to 1.863 Ma on their date model; therefore, not "fresh" in common terms. They suggested more extreme peaks of both salinity and dilution at other times.

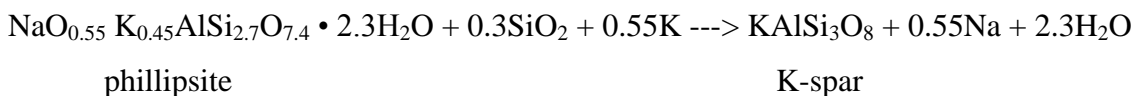
Hay (1963) cited Di Piazza et al.'s (1959) 64-day experiments in sealed bombs with trachyte and nepheline at accelerated, simulated current Olduvai conditions of 95-100°C and essentially atmospheric pressure. Trachytic glass altered (20%) to phillipsite in 20% sodium

carbonate [Na₂CO₃] solution (pH 10.3) and less easily (10%), but well, in dissolved trona [Na₃(CO₃)(HCO₃)•2H₂O] (pH 12.3). He stated that zeolites form in Olduvai soils in preference to clays. At that time was he unaware of zeolites forming on arid lands and above the water table. He posited that: 1) zeolites should be ubiquitous in arid / semi-arid climates in saline / alkaline environments and 2) and could simultaneously form where calcrete forms. By 1964, Hay remarked that tuffs could form phillipsite in a few hundred years with total alteration in thousands. Optimum conditions would be pH >9 and ratios of 10 < Na / K < 50 (may be interpreted as 0.10 > K / Na > 0.02). Hay (1963) remarks that phillipsites in Olduvai Bed V completely formed in the past 8,000-20,000 years, as a further basis for claiming fast formation. Among associated authigenic minerals are: analcime, K-spar, and dawsonite. He further reports weathering hydrolysis experiments with rhyolite tuff glass and dissolved Na₂(CO₃) at concentrations of 20%, 10%, and 5%. They produced phillipsite >> analcime, phillipsite >> chabazite, and phillipsite only, respectively.

References citing association affinity of phillipsite with K-feldspars include, among others: Hay (1963, 1964 and 1970), Larsen (2008), and Sheppard and Gude (1968). Hay (1970) provides two likely reactions:

Trachyte glass + H₂O ---> Phillipsite

and



Baur and Fischer (2002) list three ammonium phillipsites in their compendium of zeolites: (NH₄)_{3.40}Na_{0.40} · Al_{3.80}Si_{12.16}O₃₂ · 7.8H₂O; (NH₄)_{4.40}Na_{0.20} · Al_{4.41}Si_{11.60}O₃₂ · 8.1H₂O; and (NH₄)_{5.04}Na_{0.60} · Al_{5.90}Si_{10.00}O₃₂ · 9.1H₂O. Gottardi and Galli, cited in Jakkula (2005), provide cation exchange rankings for natural phillipsite: Cs ~ Rb ~ K > NH₄⁺ > Na > Li and Ba

> Ca ~ Na ~ Sr. Dwairi (1998) found that a Jordanian phillipsite exhibited consistently higher selectivity for NH_4 than for Na at three isotherms, 20, 35, and 50°C, though decreasing somewhat with rising temperature. He found that his results matched the work of other researchers. The lower end of the temperature range to be expected at Olduvai Gorge would fit in Jakkula's lower experimental range and cooler, where NH_4 exchange is most enhanced over Na.

Deocampo (2004b) states that regional, modern, saline / alkaline lakes have Na^+ and CO_3^{-2} dominating as Ca^{+2} and Mg^{+2} are removed by mineral precipitation, while SO_4^{-2} and Cl^- proportionally increase with loss of the carbonate ion. The fate of carbonate ions in soil depends on a number of factors, foremost among which are concentration and system pH. Carbonate anions form from atmospheric, organic, and inorganic origin CO_2 and water reactions. Sikes and Ashley (2007) summarize literature regarding pedogenic CaCO_3 and relate it to Bed I Tuffs IB through IF. It typically arises from cation reactions with carbonate anions and migrates downward with natural water percolation. Supersaturation resulting from evapotranspiration results in precipitation of crystalline carbonates in the unsaturated zone. It can also form and be transported in groundwater and cycle vertically with water table level changes (normal downward eluviation plus upward migration). This can lead to precipitation in the capillary fringe, as the water table responds to rainfall and piezometric surface movement. They refer to meters-thick calcrete deposits.

Studying zeolites at Hay's (1976) Locality 45 in the southeastern portion of the Paleolake Olduvai Basin, Mees et al. (2005) state, "Phillipsite formed at a later stage, from more evolved solutions, with higher K/Na ratios than during chabazite formation." They assert that water composition affected zeolite mineralogy variability. They further say that early diagenesis of Bed I lake margin deposits occurred in conditions of relatively low salinity / alkalinity upon

deposition and shortly thereafter. Then pore water was replaced by higher K/Na ratio pore water. (Lower Na / K water in Hay's (1963) terminology above.) Their article states that analcime-dominated systems followed by high Na systems are often indicative of lateral phenomena. (Interpreted as extensive, alternate wetting and drying of low slope margins with modestly changing water levels.) They report this effect to have been abrupt at Olduvai, rather than resulting from gradual water composition changes.

Jones et al. (1977) remark that most East African basins simultaneously produce clays, Ca and Mg mineral precipitates, alkali carbonate, chloride, and maybe sulfate brines, but chemical reduction removes SO_4^{-2} . If sulfate was reduced, NH_4 could have been produced from organic materials above and below tuffs. They also differentiate five stages of concentration factors: "dilute streamflow" (1), "dilute ground water" (28), "saline ground water (or hot spring reservoir)" (870), "saturated brines" (7600), and "residual brines" (16,000). These reflect existence of a very wide range of solution ionic strengths for driving a variety of authigenic reaction combinations. These could be reasonable analogs for conditions in this study's timeframe. Their modern dilute streams in the Lake Magadi area have total dissolved solids concentrations in the order of 67-384 mg/l, and all but one dilute ground water have 152-922 mg/l; fairly common worldwide values. Warm and hot lake spring concentrations ranged from 10,000 to 38,000 mg/l. Main Lake Magadi brines, in today's dry period, ranged 78,000-124,000 mg/l. Borehole brines were a bit lower, but similar. The point is "dilute" and "strong" are quite relative terms. As a point of reference, modern seawater has on the order of 35,000 mg/l total dissolved solids.

Triangular diagrams are common for portraying relationships between compositions of rocks and minerals. Robinson and Leake (1975), discussing use of AFM triangular diagrams for

study of sedimentary rocks, warn that one cannot assume close correlation for evaluating sediments' original magmas. However, this study will use the basic technique, but for other purposes and other component species in doing tuff analyses. Additional observations used Munsell soil color charts to see if there might be useful color signals regarding tuff composition. Hay (1976) and Hay and Kyser (2001) recorded sediment colors but did not mention specific use of color standards.

1.6.6 Age Research and Modeling

A century of research on Olduvai Gorge has been generating a body of literature containing many age models for placing studies in parallel. They often mismatch. For work at Loc 80 alone, many publications contain age scales, others use depth of samples from the bottom of Bed 1 Tuff IA datum upwards, and some use both to aid visualization and correlation with other studies. With passage of time, new age measurements have become available, so there is drift in the meaningfulness of each age model. Therefore, this review will not attempt to analyze that rich literature. Berry's work, upon which this research builds, used a model primarily matched to depths keyed to Hay and Kyser (2001) for Tuffs IA, IB, and IF and to their non-tuff sedimentation rates of 1 m = 5900 yr for Bed 1 units 1 and 2 and 1 m = 8300 yr for Bed 1 units 3 and 4 from paleomagnetic stratigraphy in which the Olduvai "normal" subchron lies. Deino (2012) produced new $^{40}\text{Ar}/^{39}\text{Ar}$ radiogenic dating of Olduvai sediments, revising and refining several ages and confidence limits. His work facilitated the age model construction for this work. Owing to an accident of timing, Berry (2012) had to use literature values that did not quite fit Deino's new age anchor points and conclusions for reconciling others' age values. Appendix C contains four sub-appendices: age model summary data and results, basis for computations, computations and additional notes, and a final graphic model.

One issue in building a timescale to fit a large number of sample depths is the need to account for the sedimentation intervals required for accumulation of naturally compacted non-tuff deposits between tuffs. Another is that there are several unnamed tuffs to be accounted for. More details will be presented under Methods. Deino provided estimates of new sedimentation rates: Tuff IA-IB, 22 cm/ky; Tuff IB-IE, 11 cm/ky; and IE-IF, 9 cm/ky.

Critical other information from two unpublished documents: Photocopy of typed sample number / depth tabulation for 1999 Olduvai stratigraphic column (Ashley, undated); and Photocopy of unpublished, annotated Olduvai Gorge Locality 80 Bed I field note stratigraphic column (Ashley, et al., 1999).

2. METHODS

2.1 Samples

Tuff deposit samples for analysis were collected as splits from larger samples taken at Locality 80, Olduvai Gorge, Tanzania by Gail M. Ashley (Rutgers University), Richard L. Hay (University of Arizona), Robin Renaut (University of Saskatchewan), and Godwin Mollel (Rutgers University) in 1999 and archived by Dr. Daniel M. Deocampo at Georgia State University with the same label designations (GA-L-No. -99), where they have been used in other investigations.



Figure 9 Portion of the Loc 80 30 m high sampling trench (Ashley, 1999)

The original total body of samples numbered 179 of which 25 are Bed I tuffs studied for this report. Table 3 (Results) gives sample numbers and elevations above the Bed I Tuff IA base, as the datum (smallest numerical value is the oldest, deepest below ground surface). Current sample holdings consist of 167 labeled, bagged chunks and vials of powders previously prepared by Berry (2012) for X-ray fluorescence (XRF) analysis. Some samples are not represented in this archive.

All bulk samples have been air-drying for over a decade in zip-closure plastic bags. Most powdered samples had been further air-dried during mortar and pestle grinding and storage for 1-2 years. Some additional powders were ground from original samples or reground by mortar and pestle to obtain adequate quantities and to ensure sufficient grain size reduction and mixing for XRD analysis.

2.2 Age Model

2.2.1 Preliminary Remarks

A new age model was developed for this work, because: 1) Deino (2012) published new $^{40}\text{Ar}/^{39}\text{Ar}$ analyses and age arguments superseding those in prior literature, 2) the literature is not consistent in using either sample ages or depths to portray results, and 3) it was not possible to fully validate and compare the depth/age models others had used for the same stratigraphic column. A new model was developed in an attempt to put the data in one internally consistent form. Appendix C.4 is a plot of Depth vs. Age for specific use with Locality 80 samples. However, the ages picked from that chart could be used with the original stratigraphic column to assign ages to corresponding tuffs, clays, and other sediments identified in that column originally constructed by Ashley, et al. (1999)

Berry (2012) used an age model that depended upon older radiometric and magnetochronology data and their resulting sedimentation rates for periods between tuff depositions. Table 2 summarizes Deino's (2012) results used in this study, with comparative notes. Appendices C.2 and C.3 give a complete display of the computation process generating Appendix C.4.

Table 2 Bed I tuff ages and sedimentation rate multipliers (Deino, 2012)

Tuff	Age (Ma) or Sed. Rate	Range (Ma)	Notes	Other Sources
Tuff IA	Consensus value = 1.920		1.918 = Deino measured	¹ 1.92; falls in error range
IA to IB Sed. rate	22 cm/ky		Non-tuffs	¹ 17 cm/ky
Tuff IB	1.848	+/- 0.003		
IB to IE sed. rate	11 cm/ky		Non-tuffs	
Tuff IC				
Tuff ID	1.839	+/- 0.011	Interpolation using sed. rate 11 cm/ky	
Tuff IE	1.831	+/- 0.004		
IE to IF sed. rate	9 cm/ky		Non-tuffs	¹ 12 cm/ky
Tuff IF	1.803	+/- 0.002		
¹ Hay and Kyser (2001)				
For comparison, one Bubnoff Unit of erosion or deposition = 10 Ky/cm (Bates and Jackson, 1984)				

2.2.2 Age Model Detailed Discussion

Age computation for samples not assessed by Deino was difficult owing to the following factors. The primary issue was that the stratigraphic column is of necessity broken into separate segments by the specific tuffs he analyzed. That required use of three empirical depositional rates to interpolate sample-depths / ages for non-tuff lacustrine and eolian sediments. Those graphically estimated rates had to be subjected to forward and backward iterative computations to check for consistency with deposits' physical relationships. A number of primary depth measures in the stratigraphic column did not match the Ashley (1999) typed tabulation, suggesting possible transcription errors. All depths were re-scaled and revisions used in cases of discrepancy (Table 3).

Table 3 Required stratigraphic data adjustments

Deino (2012)	Sed. Rate factor	Interval	Disposition	
	22 cm/ky	IA to IB	Changed to	23.7 cm/Ka
	11 cm/ky	IB to IE	Kept & used	
	9 cm/ky	IE to IF	Kept & used	
1999 Strat. Column	Sample No.	Depth (m) Transcription	Column Re-scaling (m)	Correction (+/- m)
	GA-L-153-99	27.50	27.40	-0.01
	GA-L-151-99	27.10	27.15	+0.05
	GA-L-38-99	26.80	26.67	-0.13
	GA-L-39-99	26.75	26.61-26.67 thick	-0.14
	GA-L-52-99	24.55	24.53	-0.02
	GA-L-53-99	24.40	24.39	-0.01
	GA-L-57-99	24.05	24.00	-0.05
	GA-L-64-99	22.80	22.71	-0.09
	GA-L-67-99	21.73	21.87	+0.14
	GA-L-145-99	19.80	19.6-19.71 19.8 puts L-145 partly inside L-146	-0.20
	GA-L-100-99	16.00	16.05	+0.05
	GA-L-97-99	15.90	15.82	-0.08
	GA-L-95-99	15.70	15.56	-0.14
	GA-L-92-99	15.05	15.09	+0.04
	GA-L-128-99	11.30	11.40	+0.10
	GA-L-126-99	11.05	11.11	+0.06
	GA-L-124-99	10.90	10.74	-0.16

A false sense of precision and accuracy had to be accepted for practical purposes.

Achieving a logical, relatively smooth curve of depth vs. age (Appendix C.4) required using an inappropriately large number of significant places (four) in computations. Significant figure sensitivity tests led to two other adjustments to make the depth vs. date curve functional. First, despite normally observed restrictions, using three decimal places (when only one or two were mathematically appropriate) separated many sample points that would have obscured each other contrary to physical reality. For the graph, three sets of tuff samples, each having the same computed dates for the set, could be and were represented by only the most appropriate one sample with respect to the geologically instantaneous deposition criterion. Thus, the curve uses

only 19 of the 25 tuff samples. This technique prevented EXCEL from making meaningless stepwise twitches in the curve, which would have subverted the sedimentation rate factors and made the curve useless for converting between depths and ages.

Tuffs IC?, ID?, and IE vitric? were used as labeled in spite of the ?-marks on the field-note stratigraphic column, because their sequence and spacings matched.

Deino's tuff ages formed the basis of an EXCEL spreadsheet filled-in to include all Bed I tuffs from elevations above datum of 3.20 to 27.40 m (IA-IF) labeled in the stratigraphic column (Ashley et al., 1999). According to standard practice, any given tuff was assumed to have accumulated instantaneously regardless of thickness. All other sediments were assumed to accumulate at one of three rates defined by Tuffs IA to IB (23.7 cm/ky), IB to IE-vitric (11 cm/ky) and IE-vitric to IF (9 cm/ky). See Results, Age model for justifications. In the absence of more detail, five instances on the stratigraphic column of wavy and dotted lines indicating probable discontinuities had to be disregarded, assumed as trivial in time (Table 4). Sample GA-L-64-99 was a tuff for which thickness was assumed irrelevant according to the zero-duration criterion.

Table 4 Possible intra-Bed I discontinuities

Related Sample Number	Approximate Depth, m	Age, Ma	Maximum Amplitude, m
GA-L-26-99, top	5.2	1.915	
GA-L-121-99, top	10.1	1.896	
GA-L-122-99, top	10.4	1.894	
GA-L-81-99, top	13.9	1.879	0.13
GA-L-64-99, top	22.95	1.842	Tuff blocks possibly re-worked

The closure criterion was tested and accomplished by computing from the two independent bases of Tuff IA and Tuff IB toward the middle, rather than from one to the other.

Whenever possible (most cases) each computed age was independently calculated from a specific, Deino (2012) dated tuff; i.e., IA, IB, ID, IE, or IF. That forestalled cumulative errors that would have arisen from serially calculating ages one from the other.

"What if" computation checks and sequence logic ruled out some incorrect possibilities and led to discovery of the noted anomalies in originally-typed tabulated depths; e.g., tuff sample GA-L-145-99 cannot lie partially within non-tuff sample GA-L-146-99, and seven beds were listed as much as 1 to 2.0 decimeters too thin or thick. Ages computed to compensate for those anomalies dramatically smoothed the otherwise choppy depth vs. age correspondence curve (see Results). That curve can be used to assign ages to non-tuff beds. These improvements were accomplished simply by careful selection of computation origins, error correction, and sensitivity verification with due diligence to let numbers fall where they naturally would, not by force fitting or selective data-point choice.

2.3 Analytical Methods

2.3.1 X-ray diffraction (XRD)

XRD analysis determined the primary and second-rank minerals present in Bed I tuffs. The equipment used was a PANalytical X'Pert Pro X-ray diffraction unit with $\text{CuK}_{\alpha 1}$ radiation with a wavelength of 1.5406 Å, operating at 45 Kv, 40 mA, and fitted with a reflection transmission spinner. Sample vials were shaken and rotated several times in all three axes to remix the material after storage and handling. Sample holder rings were inverted on a deeply scored glass plate (to ensure a random reflection powder exposure), almost filled with free-poured sample powders, and gently "closed" by placement of the inverted holder base on top. The entire assembly was then carefully lifted without sliding the parts and returned to the upright position with the sample exposed (glass gently removed). If sample stuck to the scored plate or

the plate moved in handling, the sample was returned to its vial for re-mixing and re-sampling. Figure 10 shows the system with a sample in-process. Diffraction scans were about 15 minutes at “normal” resolution (0.001° , stepwise). Samples were scanned from $2\text{-Theta} = 5^\circ\text{-}60^\circ$.

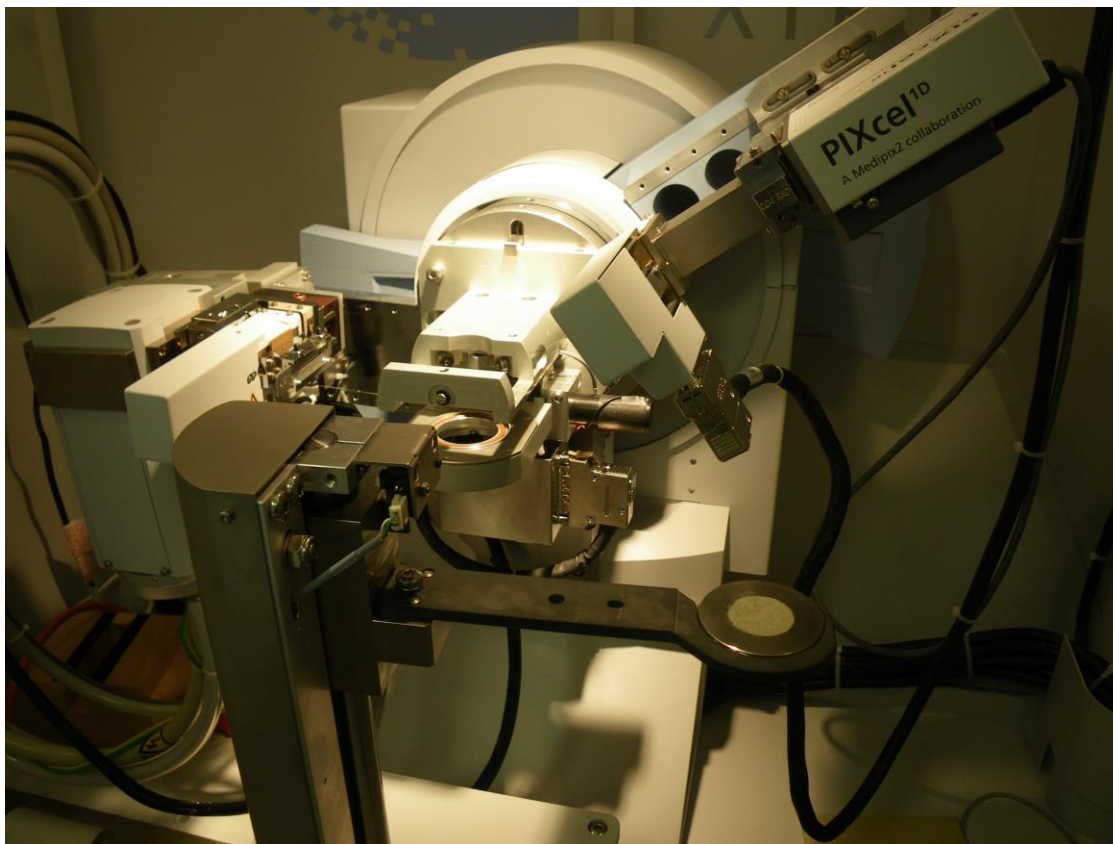


Figure 10 XRD system with the sample loading on the reflection transmission spinner

This data set comprises 25 samples. Four additional tuffs identified on the field stratigraphic column could not be represented, because no samples exist: 8.83 m, no name / no sample; 8.97 m, no name / no sample; 20.64 m, GA-L-150-99, no sample; and 27.20 m, GA-L152-99, no sample.

Analysis used PANalytical Data Collector, DataView and HighScore Plus software to record, access, and manipulate diffraction data. HighScore used software-produced scores to identify the predominant minerals in samples. However, it was also usually necessary to do "what if" trials with the two to five highest scoring minerals in each sample. The result was not

always identical to the algorithm's criteria. Results reported are the software-identified candidate minerals that satisfied the most chart peaks with the fewest minerals (Ockham's razor principle). Some XRD peaks went unused, rather than force minerals to fit when using them led to obviously strange choices for the geochemical situation. Figure 11 illustrates how XRD peaks for sample GA-L-61-99 were "optimized" to a minimum of most prominent minerals. In this case, very few, minor peaks were not assigned to a mineral by HighScore after sensitivity trials.

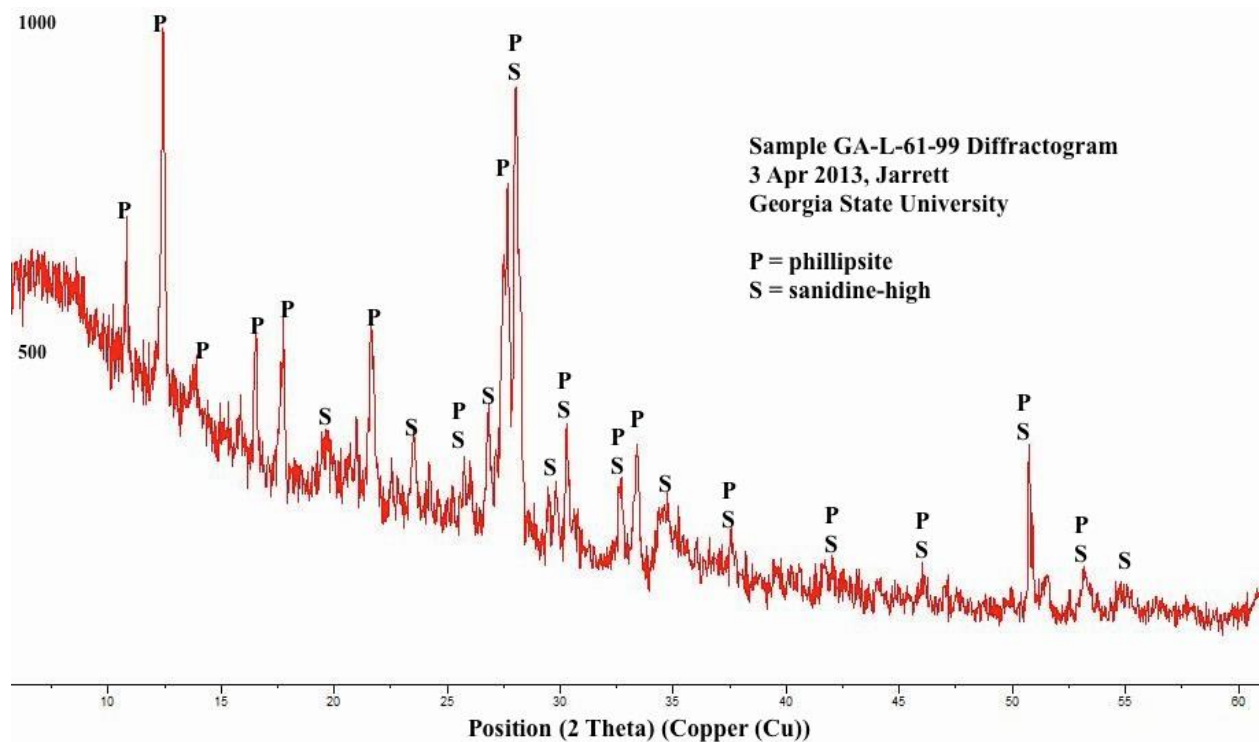


Figure 11 Sample diffraction scan: Locality 80 Tuff ID sample GA-L-61-99, 1.839 Ma

2.3.2 Re-analysis of X-ray fluorescence (XRF) Data

Berry's (2012) XRF data for oxides (Appendix A) were processed to plot binary and triangular relationships for the tuffs in this study for comparison with XRD findings. Some groupings had to be re-normed to 100% from Berry's data for the various oxide and oxide ratio plots.

2.3.3 *Munsell Color Comparison*

Powdered samples were viewed with a fresh (purchased 2013) Munsell Soil Color Chart book (2009). Colors were examined in natural, northern exposure light and recorded for comparison with XRD and XRF data. Schaetzl (2005) provides instructions on reading and interpreting colors. Given the age of Loc 80 samples and their long desiccation in storage, the recommendation that readings be taken at "soil-moist conditions" could not be followed.

2.3.4 *Statistical Analysis*

SPSS Version 19 (2010) examined possible dichotomous distributions, a relationship first noticed in color assessment data then in XRD analyses. Dichotomous discriminant analyses were performed in listwise and stepwise modes for SiO₂, Al₂O₃, MgO, CaO, Na₂O, K₂O, and (Na₂O+K₂O) around an age gap, 1.869 to 1.857 Ma defined by a subjectively noted change in mineral authigenesis. "Dichotomous discriminant" relates to classifying a total population into two groups for comparison to estimate whether a hypothesized commonality exists or not (Agresti, 1996). This technique can test whether preconceived non-metric groups are distinct for a particular "categorical dependent variable" considering all of the independent variables. It was desired to know whether two distinct groups might exist, based on constituent cations as predictor variables. The test can be run in listwise and stepwise modes. Listwise mode analyses the entire data set in search of grouping. Stepwise mode selects the most correlated independent variable, computes its contribution to categorization / classification of the sample group members, and works progressively through the remaining input variables to determine which contribute most to predicting the dependent variable. These tests are suitable for small sample sizes.

3. RESULTS

3.1 Age Model Reconciliation

Tuff depth-age Appendix C provides a graphical scaffold for estimating other ages according to depth, specifically at Loc 80, and possibly extendable to the same beds at other locations. Properly addressing realities of sample collecting and of recently augmented, re-analyzed, and summarized geochronological knowledge (Deino, 2012) was complex and time consuming. In testing proposed non-tuff sedimentation rate factors, it verified two and modified a third. And, it revealed inconsistent sample depth reports for correction. The sampling depth vs. conversion age curve, Appendix C.4 is imperfect, with some wobbles. One would expect to see straightness, when using three line segment slopes, but the imperfections reflect the discipline applied to extrapolating away from the firmest ages in toward each other, not to force fit points to lines drawn between firm end-dates. The rather good closure of those extrapolations within the respective data intervals suggests that the results are fairly reliable, as no effort was made to make things fit, *per se*. That is, numbers were not rounded, tweaked, or discarded to achieve a "desirable" outcome. Rather, iterative computation checks and crosschecks, chronology logic checks, and data error corrections progressively cleansed the data and process. Deino (2012) proposed a sedimentation factor of 22 and latter suggested trying 23 cm/ky (Deino, 2013) for the interval Tuff IA to IB. The value 23.7 cm/ky worked better. Trial calculations above and below 23.7 cm/Ka at 23.6 and 23.8 resulted in distortions, but further, micro adjustments in a second decimal place around 23.7 cm/Ky were not tried, as being indefensible.

3.2 Tuff Mineralogy

3.2.1 *X-ray Diffraction (XRD)*

Mineralogical findings comprising Table 5 below are the central summary of outcomes for this project and for understanding results and discussions that follow. Calcium and magnesium-bearing minerals (Table 5) dominated tuffs deposited from 1.920 Ma until 1.893 Ma. At that point XRD outputs show authigenesis of high-K minerals starting early, from 1.891 Ma through Bed I until 1.803 Ma, a period of almost 90,000 years. An overlapping period of high-Ca and Mg-bearing mineral deposition occurred from 1.891 Ma to 1.869 Ma. Na-rich minerals appear as primary and second rank minerals at odd points along the entire timeline. Phillipsite is not seen as a major first or second rank mineral through 1.869 Ma, and is prominent from 1.857 and onwards through the final deposition of Bed I. Of the ten tuffs deposited from then until 1.803 Ma, phillipsite was the main mineral in six and the second mineral in a seventh. Ca was also significant in Tuff IE in this later period.

3.2.2 *Re-analysis of X-ray Fluorescence*

Comparing Table 5 data with Berry's (2012) chart (Figure 7) regarding relative salinity / dilution according to meteorological cycles, but expressed in descriptive terms for tuff samples at corresponding ages, reveals phillipsite formed in these regimes: "dilute" (4 times), saline / alkaline (2 times), and transitional from saline to "dilute" (1 time) for a total of seven. The latter, Tuff IE vitric in the transitional regime at 1.835 Ma, showed phillipsite as a significant second score mineral.

Table 5 Tabular age model and summary XRD output

NH4 and Mg in phillipsite refer to mineral varieties with strong peak correspondence identified by HighScore. These have not been verified.

Sample ID, GA-L-x-99	Depth from Bottom	Mod. Deino Date (Ma)	Tuffs	Highest Score Mineral	Second Score Mineral(s)	Environ. (Berry, 2012)
153	27.40	1.803	Tuff IF	phillipsite (NH4)	sanidine	sal/alk
151	27.15	1.803	Tuff IF	f-spar sanid.-like	none	sal/alk
52	24.53	1.831	Tuff IE	phillipsite (NH4)	calcite	dilute
53	24.28	1.831	Tuff IE	orthoclase	calcite	dilute
54	24.24	1.831	Tuff IE	phillipsite (NH4)	f-spar sanid.-like	dilute
57	24.00	1.835	Tuff IE Vitric?	anorthoclase	phillipsite (Mg)	entering dilute
61	23.40	1.839	Tuff ID ?	phillipsite (NH4)	high sanidine	sal/alk
64	22.71	1.843	Tuff IC ?	f-spar sanid.-like	bloedite	entering sal/alk
67	22.00	1.848	Tuff IB	phillipsite (NH4)	sanidine	dilute
145	19.60	1.857	Tuff	phillipsite (Mg)	albite	dilute
104	16.70	1.869	Tuff	orthoclase (K 0.94)	anorthite (sodian)	entering sal/alk
100	16.05	1.871	Tuff	sanidine	calcite	dilute
97	15.82	1.872	Tuff	f-spar sanid.-like	calcite	dilute
95	15.56	1.873	Tuffs / clays	interm. microcline	anorthite calcite	dilute
92	15.09	1.875	Tuff	calcite	hydrotalcite	dilute
85	14.20	1.878	Tuff	sanidine	jarosite	interm. dilute
128	11.40	1.890	Tuff	f-spar sanid.-like	hydrotalcite	dilute
126	11.11	1.891	Tuff	sanidine (high)	bloedite	dilute
124	10.74	1.893	Tuff	calcite	gypsum	dilute
117	9.45	1.898	Tuff	gypsum	none	dilute
24	4.95	1.916	Tuff	ankerite	anorthite	entering sal/alk
19	3.87	1.920	Tuff IA	calcite	orthoclase	entering sal/alk
18	3.60	1.920	Tuff IA	analcime	dolomite	entering sal/alk
17	3.40	1.920	Tuff IA	calcite	analcime	entering sal/alk
16	3.20	1.920	Tuff IA	calcite	dolomite	entering sal/alk

These XRD results do not show consistent zeolite authigenesis cycles in the tuffs. Neither phillipsite nor other zeolites appear firmly tied to the presumed strongest saline / alkaline waters. Sanidine and sanidine-like feldspars seem to have formed from tuffs mostly in "dilute" waters, but not exclusively.

A tendency is seen for high phillipsite tuffs to alternate with K-spar tuffs, even when supposedly deposited almost contemporaneously. It was noted in Introduction that trachyte glass → phillipsite → K-feldspar (Hay, 1963, 1964 and 1970; and Sheppard and Gude, 1968), but the alternations are regular in these deposits, as though there were short cycle condition changes not seen as cycles in Table 5.

Careful taking of tangent points at peaks and center points of transitions (inflections) from Figure 7 yielded Appendix E used to plot Figure 12. Caution is required here, because the Berry (2012) source curve was not statistically rigorous, and these secondary peak and inflection data were taken visually from that curve. The portrayal is largely notional, but the gross temporal relationships are clear. With the exception of four tuffs clustered at 1.920 Ma at a climate inflection and the two extreme, extrapolated wet cycle points, four periods occurred when climate moved from driest to wetter followed shortly by increases in volcanic activity.

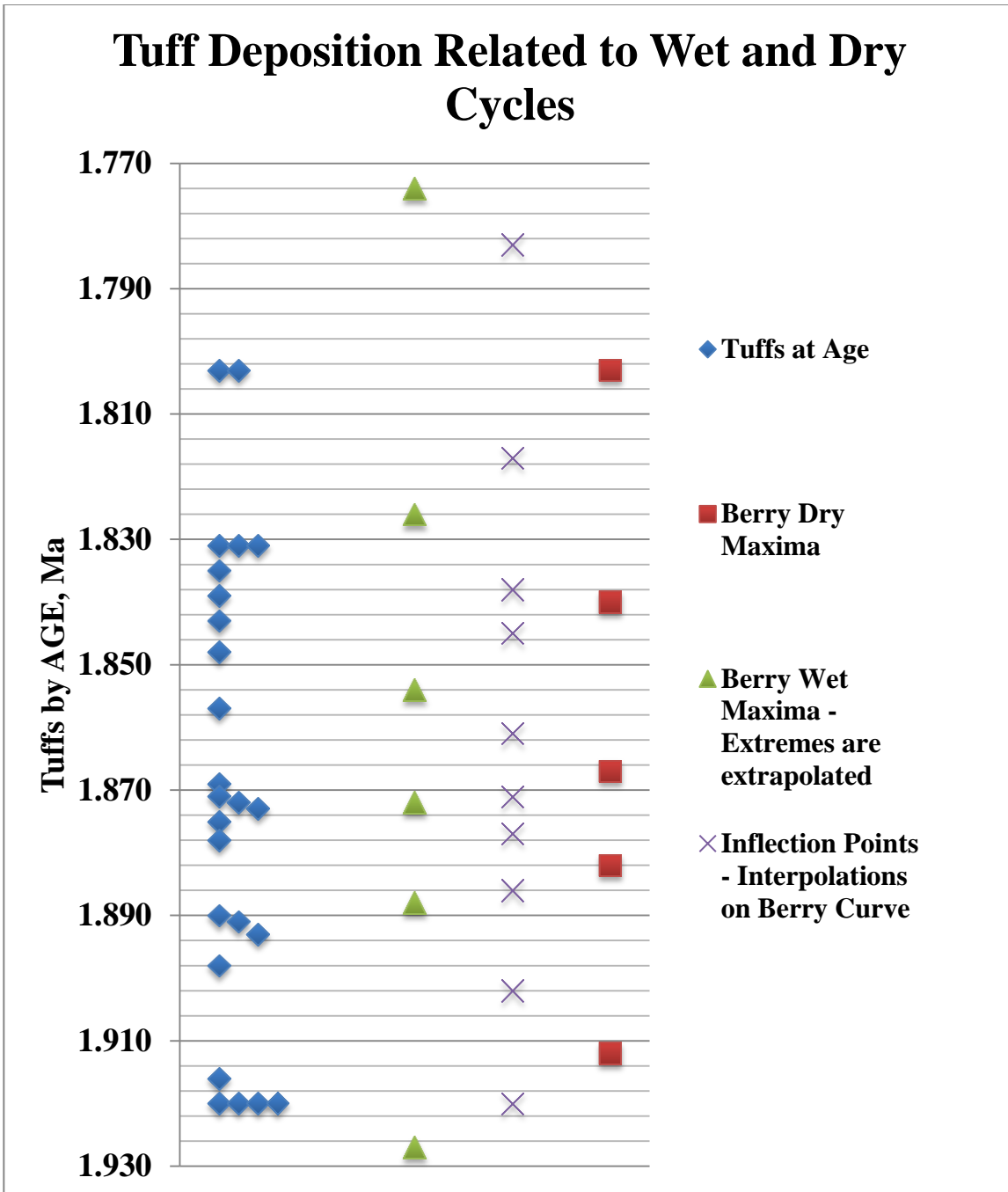


Figure 12 Tuff deposition history related to Berry (2012) wet and dry cycles
Berry's curve salinity maxima, inflections, and minima are plotted against the new age model.

While each of the next seven analyses through paragraph 3.2.4, Tuff Color, taken separately, is statistically very weak, a definite pattern will be seen.

Examination of alkali metal ($\text{Na}_2\text{O} + \text{K}_2\text{O}$) values compared to alkaline earth metal CaO divided by MgO (as a weathering index) in Figure 13 matches expectations based on molecular composition that phillipsite-bearing Bed I tuffs should be high in Na and K.

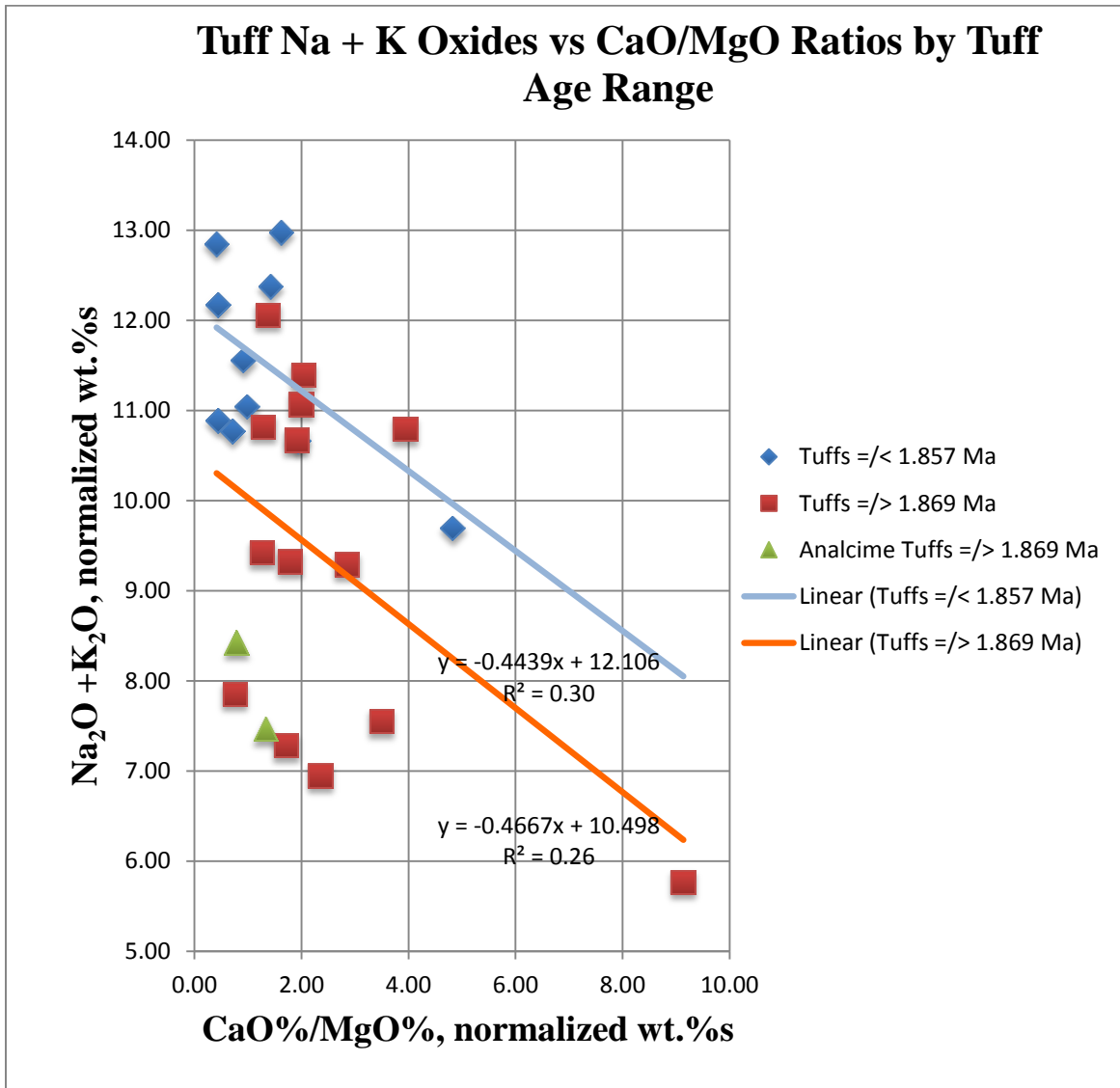


Figure 13 Tuff ($\text{Na}_2\text{O} + \text{K}_2\text{O}$) oxides vs. CaO/MgO ratios: Phillipsite vs. non-phillipsite tuffs

Older tuffs, including the two analcime-containing tuffs, tend to be correspondingly higher in alkaline earth elements. The contrast is not extreme between the two weak regression lines; non-zeolite tuffs average only about 1.5% percent lower ($\text{Na}_2\text{O} + \text{K}_2\text{O}$) sums. However, the data scatter of both sets is quite large, and both linear regression R^2 values are low. Six of the

seven phillipsite tuffs have CaO/MgO wt. % ratios 0.4 to 1.6. For comparison, 1.4 is the theoretical dolomite ratio. Two distinct fields exist with some overlap. Both analcime tuffs are low on the alkali scale, compared to the majority of other tuffs.

Figure 14 below, with MgO as denominator on both axes, is extremely scattered and has very low R² values (a polynomial fit was the best of six methods), for zeolite, non-zeolite, and combined tuffs (latter tried, but not shown). The weight percent proportions of (Na₂O +K₂O) and CaO in the samples do not show a relationship, other than that the non-phillipsite tuffs

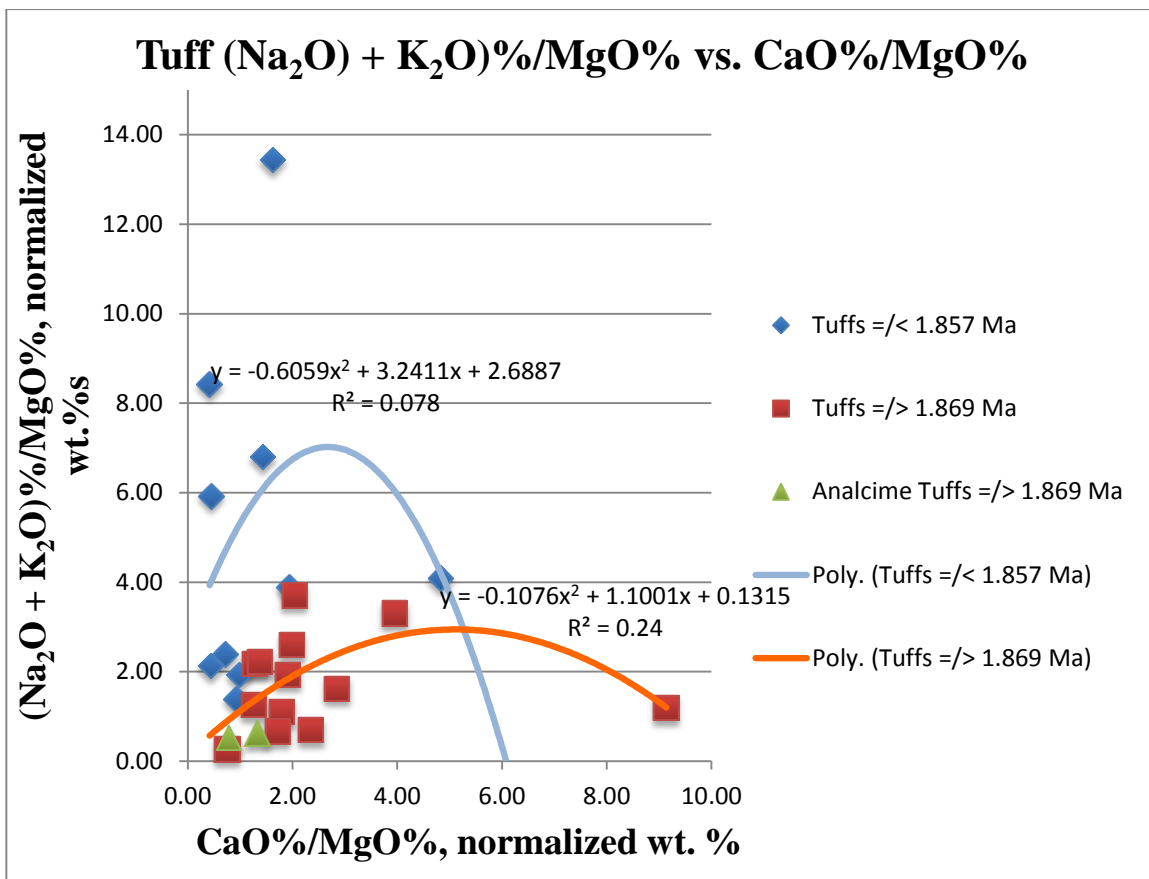


Figure 14 Tuff (Na₂O + K₂O)%/MgO% vs. CaO%/MgO%.

(those 1.869 Ma and older) are again seen higher in Ca than the younger ones, which is subjectively noted when examining Table 5 above. This portrayal shows a wider divergence between alkali content and CaO content for the young zeolite set; that is, even less correlation of Ca content with authigenesis of minerals in the younger tuffs.

Triangular plot, Figure 15, contains all 25 tuff data points. It shows all but one phillipsite tuff in the top 50% of the alkali field and at or below 50% in the CaO field. All are below 30% MgO.

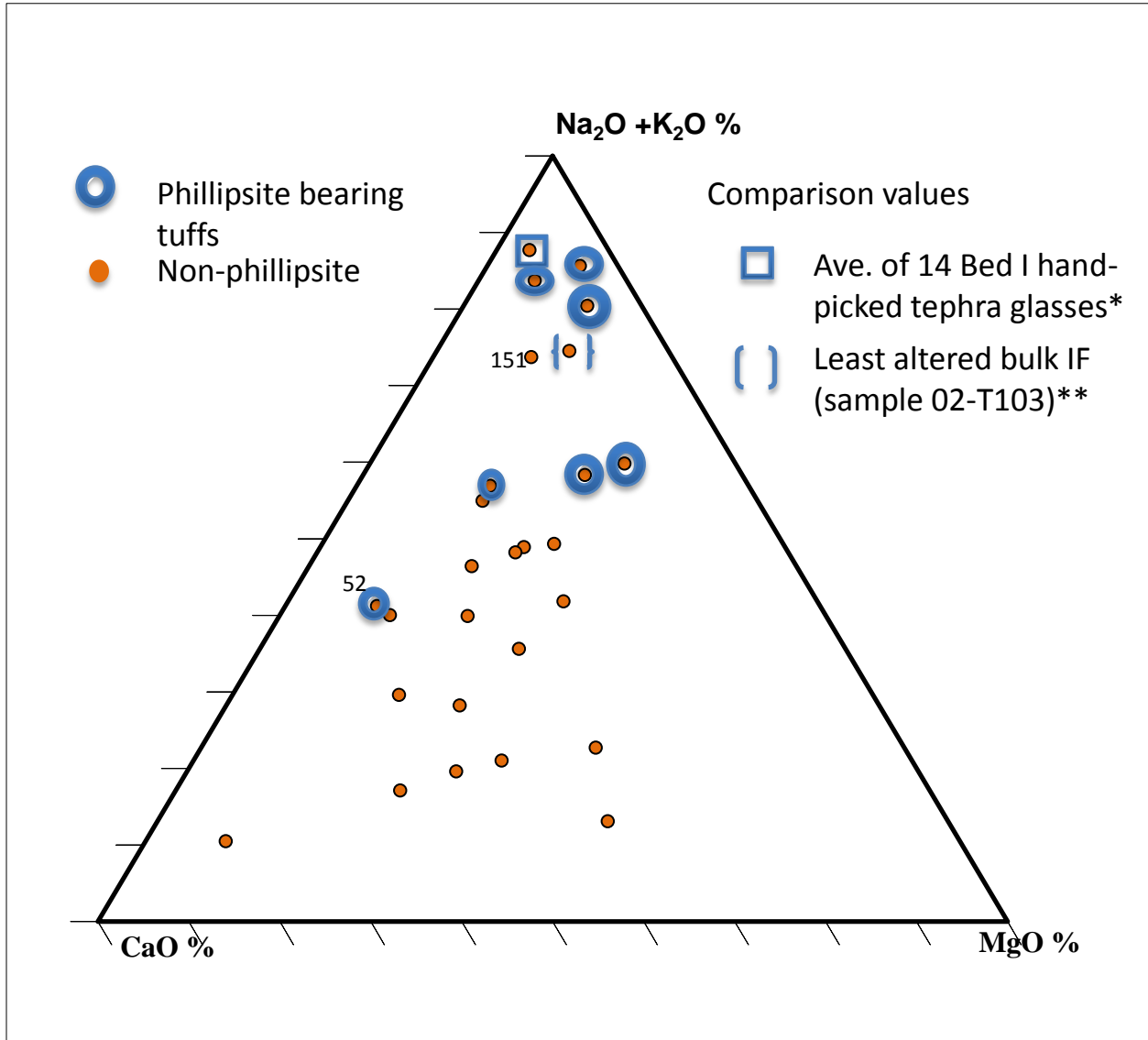


Figure 15 Triangular plot of tuff oxides
 Normed raw XRF oxide data were re-normed to 100% for just the four oxides on this chart.
 Circles enclose tuffs deposited at and after 1.857 Ma. (* McHenry, 2005); ** McHenry, 2009)

XRD data show that GA-L-52-99, a sub-bed of Tuff IE, has 49% CaO wt. %. XRD showed it having calcium-sanidine, as the second mineral after phillipsite (NH₄). The majority of

the 18 non-zeolite tuffs tend to lie toward the CaO vertex (bounded by the 30% MgO and 50% alkali coordinates) and contain much more Mg than they do alkalis.

3.2.3 Combined Findings of XRD and XRF Analyses

Figure 16 shows zeolite tuffs and cation occurrence for both zeolite and non-zeolite-bearing tuffs.

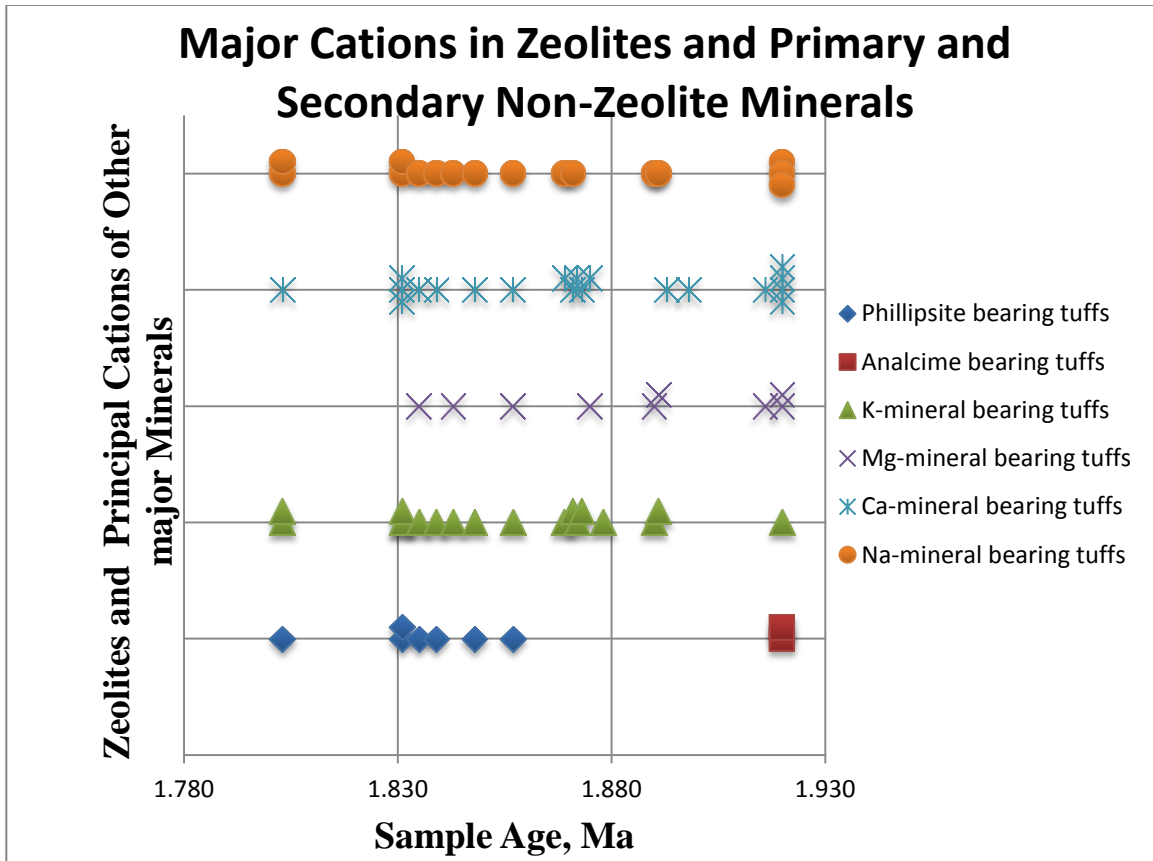


Figure 16 Major cations in zeolites and primary and secondary non-zeolite minerals. Data points were obtained by tabulating the principal non-silicon cations in all primary and second rank minerals to develop this occurrence frequency map.

Figure 17 re-examines Berry's (2012) XRF CaO / MgO oxide ratios for tuffs regarding age. While a high degree of scatter exists, the power regression curves for zeolite tuffs versus oxide ratios exhibit mirror curves. An apparent outlier at CaO / MgO = 9.14 is actually legitimate with a calcite and gypsum composition. No common regression method was particularly useful.

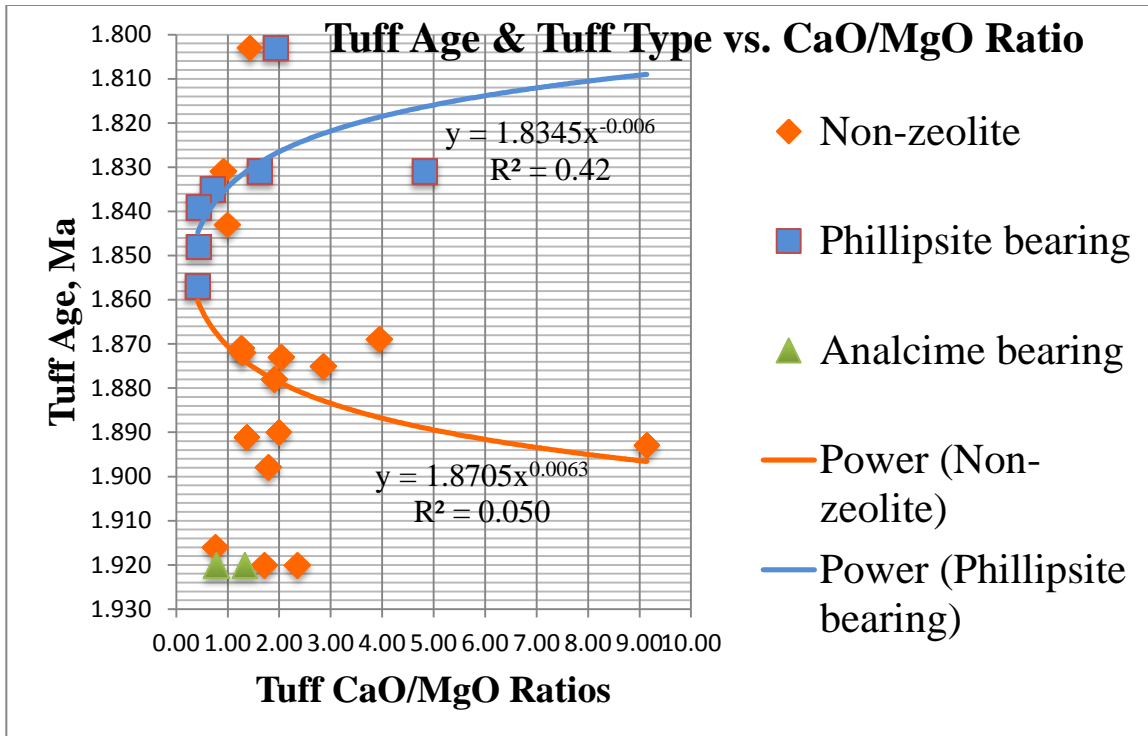


Figure 17 Tuff age & tuff type vs. CaO/MgO ratio (Appendix I)

Tuff GA-L-145-99, deposited (1.857 Ma) nine 9 ky before Tuff IB, represents the onset of major tuff zeolitization, as reported by XRD. Various potassium-feldspars first appear in the record, with tuff GA-L-126-99 at 1.891 Ma. Analcime was identified in two tuffs during presumed transitions to higher Na concentration saline / alkaline conditions in the otherwise Ca-dominated early years around 1.920 Ma.

Most zeolitization occurred (Figure 18) at an Al_2O_3/MgO ratio of 2.8 and beginning at age 1.857 Ma. Low Al_2O_3/MgO non-zeolites and zeolitization overlapped two times at or below a ratio of 3.13. The non-zeolite coefficient of determination R^2 value of 0.49 for age against oxide ratio is the highest for any of the scatter plots, but neither is strong. Once again, despite the poor to no-correlation, a population spit seems to exist.

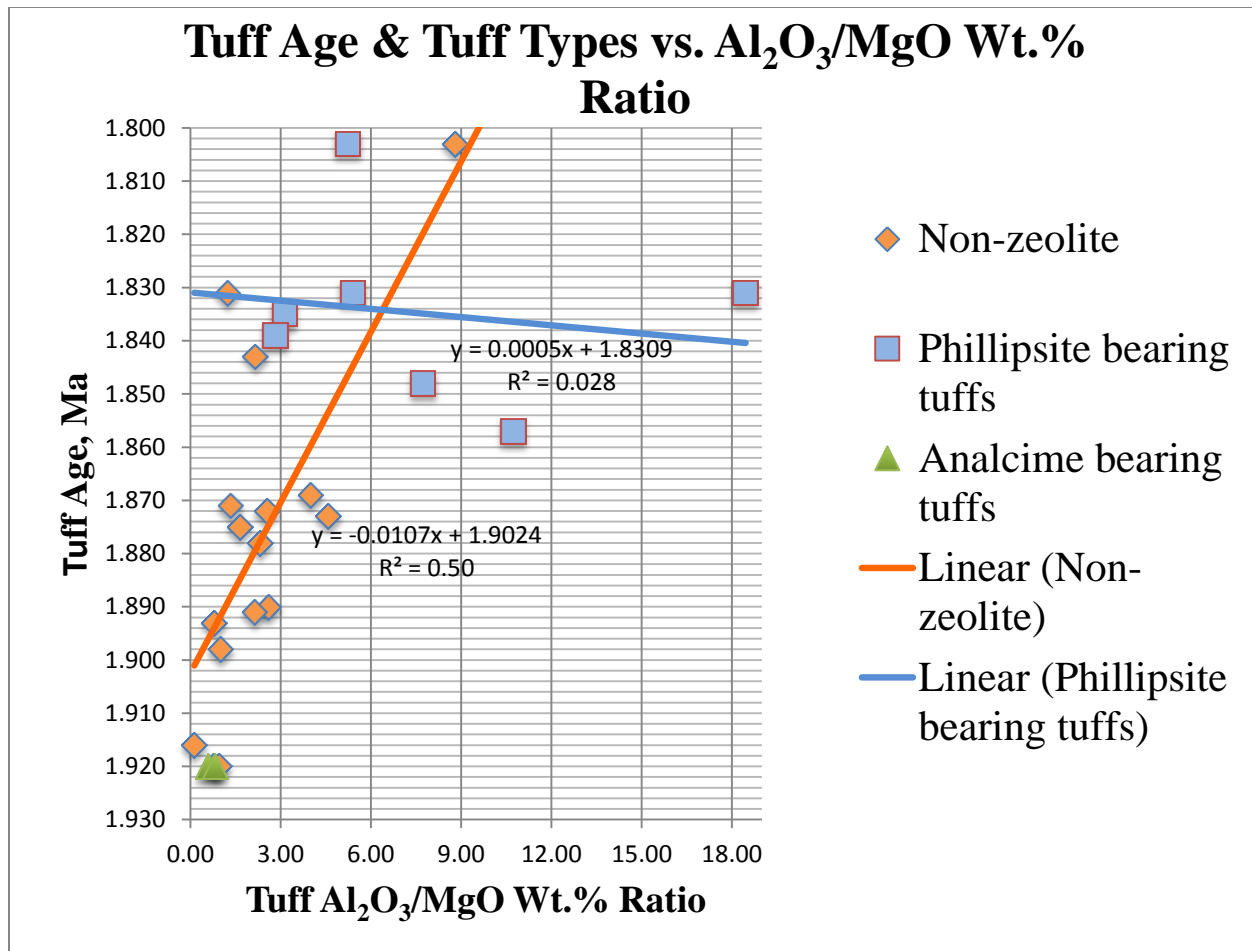


Figure 18 Tuff age & tuff types vs. Al₂O₃ / MgO wt.% ratio
Slope signs seem reversed, but are correct with the inverted ordinate.)

Deleting the outlying 1.803 Ma zeolite tuff (GA-L-151-99) made little change in the R² value or the line's location. The non-zeolite tuffs without the 1.803 Ma outlier, cover a narrow range of random-appearing values and would have an almost vertical curve.

3.2.4 Tuff Color

Table 6 augments Table 5 by adding tuffs' Munsell color codes and value/chroma pairs for comparison with tuff mineralogy. A similar break is seen on either side of 1.869 and 1.857 Ma in colors as for XRD-identified principal minerals, with a few exceptions.

Table 6 Munsell soil color Analysis

ID	Depth from Bot-tom	Jarr-Deino Age						Berry Projection	Munsell Designations	
									Code	Value/ Chroma
GA-L-x-99	Meters	Ma	Tuff	First Mineral	Main cation(s)	Second Mineral	Main cations	Environment		
153	27.40	1.803	Tuff IF	phillipsite (NH4)	Ca, Na, K, NH4	sanidine	K	sal/alk	10YR	8/4
151	27.15	1.803	Tuff IF	f-spar sanid.-like	K, Na	none	none	sal/alk	10YR	7/4
52	24.53	1.831	Tuff IE	phillipsite (NH4)	Ca, Na, K, NH4	calcite	Ca	dilute	10YR	8/3
53	24.39	1.831	Tuff IE	orthoclase	K	calcite	Ca	dilute	10YR	8/1
54	24.28	1.831	Tuff IE	phillipsite (NH4)	Ca, Na, K, NH4	f-spar sanid.-like	K, Na	dilute	10YR	8/4
57	24.00	1.835	Tuff IE Vitric?	anorthoclase	Na, K	phillipsite (Mg)	Ca, Na, K, Mg	entering dilute	10YR	8/3
61	23.40	1.839	Tuff ID ?	phillipsite (NH4)	Ca, Na, K, NH4	high sanidine	K	sal/alk	10YR	8/3
64	22.71	1.843	Tuff IC ?	f-spar sanid.-like	K	bloedite	Mg Na	entering sal/alk	10YR	7/2
67	22.00	1.848	Tuff IB	phillipsite (NH4)	Ca, Na, K, NH4	sanidine	K, Na	dilute	10YR	8/3
145	19.60	1.857	Tuff	phillipsite (Mg)	Ca, Na, K, Mg	albite	Na	dilute	10YR	8/3
104	16.70	1.869	Tuff	orthoclase (K 0.94)	K	anorthite (sodian)	Ca, Na	entering sal/alk	10YR	7/3
100	16.05	1.871	Tuff	sanidine	K, Na	calcite	Ca	dilute	10YR	7/2
97	15.82	1.872	Tuff	f-spar sanid.-like	K, Na	calcite	Ca	dilute	10YR	7/2
95	15.56	1.873	Tuff/clay	interm. microcline	K	anorthite	Ca	dilute	10YR	6/2
92	15.09	1.875	Tuff	calcite	Ca	hydrotalcite	Mg	dilute	10YR	7/3
85	14.20	1.878	Tuff	sanidine	K, Na	jarosite	K, Fe	interm. dilute	10YR	7/4
128	11.40	1.890	Tuff	f-spar sanid.-like	K, Na	hydrotalcite	Mg	dilute	10YR	6/6
126	11.11	1.891	Tuff	sanidine (high)	K, Na	bloedite	Mg, Na	dilute	10YR	8/4
124	10.74	1.893	Tuff	calcite	Ca	gypsum	Ca	dilute	10YR	6/3
117	9.45	1.898	Tuff	gypsum	Ca	none	Ca	dilute	10YR	6/4
24	4.95	1.916	Tuff	ankerite	Ca (Fe, Mg, Mn)	anorthite	Ca	entering sal/alk	2.5Y	8/1
19	3.87	1.920	Tuff IA	calcite	Ca	orthoclase	K	entering sal/alk	10YR	6/4 OR 7/4
18	3.60	1.920	Tuff IA	analcime	Na	dolomite	Mg, Ca	entering sal/alk	10YR	8/3
17	3.40	1.920	Tuff IA	calcite	Ca	analcime	Na	entering sal/alk	10YR	7/4
16	3.20	1.920	Tuff IA	calcite	Ca	dolomite	Mg	entering sal/alk	10YR	7/4

3.2.5 Statistical Analyses

An unexpected change in gross mineralogy, first noted in Table 5, then later in Figures 13, 14, 15, 17, and 18 and Table 6, was tested using SPSS Version 19 (2010). Two forms of dichotomous discriminant analysis were used to determine which elements from the oxide

dataset best predicted whether samples came from older or younger tuff bed samples.

Discriminant analysis is a form of regression analysis using a dichotomous outcome variable and a series of continuous predictor variables. Its purpose is to create an equation that can best predict whether an observation falls in one category or the other on the outcome variable. In this research, the outcome variable was sample age (splitting age data into two categories for comparison), with the division between early and later samples coinciding with the occurrence of phillipsite in the 1.857 Ma tuff. Predictor variables for listwise and stepwise analyses were SiO₂, Al₂O₃, MgO, CaO, Na₂O, K₂O, and Na₂O+K₂O. Data comprise Appendix K.1.

The first analysis entered all those predictor variables listwise, $R = .72$, $F(6, 18) = 3.20$, $p < .03$. All predictor variables except K₂O entered the equation. However, none of the other predictor variables made a significant contribution individually, because these variables are all highly inter-correlated, as shown by the SPSS correlation matrix in Appendix K.2. However, knowing the combination of the other six variables was a good predictor for whether a tuff deposited before or after 1.857 Ma.

The second analysis entered predictor variables in stepwise manner, $R = .66$, $F(1, 23) = 17.54$, $p < .001$. SiO₂ was entered into the equation first ($t = -4.2$, $p < .001$). None of the other variables added significantly to the equation because they are highly correlated with SiO₂.

The fact that Si and Al are seen highly correlated with each other in contingency table Appendix K.2, as expected by the high frequency of silicate occurrence in the general mineralogy, is a reality check. Alkali oxide sum (Na₂O+K₂O) is highly correlated with CaO and both are individually highly correlated with Si and Al. Neither Na nor K alone is so highly correlated with any other cation.

4. DISCUSSION

While this work began with one hypothesis to evaluate, results revealed additional questions for exploration, as will be seen in the ensuing discussion.

4.1 Age Model

Geological age models need to be refined in light of new information; old models remain in the literature forever and are cited, while the newest information is out of view until publication. And, authors are split between those writing in terms of empirical age measurement and those using stratigraphic depth as a time proxy for age. It is not always clear which measure is the more solid. For these reasons, this work required construction of an updated age model to portray stratigraphic and time relationships in parallel.

Though not an originally intended element of this project, the opportunity arose to test Deino's 2012 proposals with a real data set having tight stratigraphic measurement records and a clear sequence of logic built-up by highly respected researchers. Use of Loc 80 samples placed in Deino's basic framework with detailed attention to inclusion of un-named tuffs and doing both forward and back-calculations, whenever possible, generated a relatively smooth age-depth curve for proposing one new non-tuff sedimentation rate at Loc 80 in the CB and for validating two others. The outcomes are: change Deino's Tuff IA to IB sedimentation rate from 22 cm/ky to 23.7cm/ky; accept IB to IE vitric as 11 cm/ky; and accept IE vitric to IF as 9 cm/ky. These are used in lieu of Hay and Kyser's (2001) and Holdship's (1976) sedimentation rates used by Berry (2012). Stretching the limits of significant figure protocols might have added an unwarranted pretense of perfection; but, many samples otherwise would have been seen in the wrong orders and times for how they were actually found *in situ*. Asserted validity of these findings is supported by the fact that they work: segments of a plotted curve joined as almost straight lines,

in spite of some portions being calculated from different starting points. Correction of errors found in basic data during the process progressively improved the smoothness of fit and joining.

As state above, the possibility of discontinuities in Bed I adds some uncertainty to the age model. And, lack of four tuff samples (no more material seems to exist) for inclusion in XRD analysis weakened this study.

Deino's (2012) revised Tuff IF age of 1.803 Ma is significantly different from the 1.79 Ma used by Ashley (2007) citing McHenry's work in 2005; a 13 ky shift. This could materially affect some climate cycle correlations. For instance, it would not change Berry's (2012) Figure 17 curve in terms of sample depth, but it would move lake cycle 4's salinity peak in time by half of a lake cycle (13 ky / 24 ky) for that particular period. That could be significant in projecting surrounding habitat environments.

4.2 Tuff Mineralogy

4.2.1 X-ray Diffraction (XRD)

Bed I tuffs contain frequent occurrences of phillipsite from 1.857 Ma onward often alternating with K-feldspars of one variety or another (Table 5). There seems to be no consistency. There are switches even between the three Tuff IE samples. Calcium and magnesium-bearing minerals dominate from 1.803 to 1.869 Ma. It is noteworthy that calcium and magnesium minerals are also seen with phillipsites, as well as dominating in the early period. The break between 1.869 and 1.857 Ma stands out. It raises questions about what major source rock, groundwater composition or flows, or other changes might have caused such a divide. It is not clear whether authigenesis only produced phillipsite in the later period, or whether a groundwater change might have caused its destruction in the earlier period. Interestingly, These findings are inconsistent with the premise that high salinity / alkalinity is the prime criterion for

tuff authigenesis to zeolites, thence to K-feldspars, because highly concentrated waters presumably existed in the early periods, too (Berry, 2012). Phillipsite and K-feldspars occurred in similar environments both together and separately in time, agreeing with the premise that phillipsite modifies to K-feldspars. Early calcium and magnesium mineral occurrences fit with expected early precipitation in less concentrated waters (Coto et al., 2012; Deocampo, 2004b; Sikes and Ashley, 2007). Appendix D contains related mineral formulae.

Occurrence of five NH_4 exchanged phillipsites of the seven, if eventually shown valid, (two are Mg phillipsites) imply that anaerobic decomposition of biomass below tuff-falls and in other lacustrine sediments above them could have released K from phillipsite into solution for dissipation or K-spar formation, in addition to K-feldspars generated strictly by salinity / alkalinity reactions. If true, that would confound attempts to assign all K-spar authigenesis to saline / alkaline conversion of trachyte glass to phillipsite to K-spar.

Ca and Mg minerals also appear irregularly in the "phillipsite zone". Hay (1964) spoke of analcime, chabazite, clinoptilite, dawsonite, erionite, and K-spar in highly authigenic sediments. These might have been minor accessory minerals in some tuffs, but not major ones according to the identification protocol used in this work.

4.2.2 Combined Findings of XRD and XRF Analyses - Cyclic Relationship

The concept of wet / dry cycles giving rise to cycles of authigenic mineral formation in shallow, closed basins is well established in the literature. It is supported by many worldwide cases of specialized occurrence of minerals that typically form in each of Jones et al.'s (1977) five environments from fresh to "residual brines". However, review of Table 5 with interpretation of Figure 7 shows no particular connection between formation of tuff-origin phillipsite and sanidines or of their formation related to water quality when the respective tuffs

deposited into the CB. In fact, both minerals are found in both weak and strong salinity / alkalinity conditions according to Berry's cation oxide combined-data cyclic chart. Contrary to expectations, phillipsite is the primary mineral seen during four periods of a "dilute" lake, one of moving from saline to dilute, and only two in presumed dry periods of strongest salinity / alkalinity. Together, phillipsite and sanidines occur opposite water ratings of "dilute" ratings seven times and four times at strong concentrations. Those counts exclude orthoclase, microcline, and "K-feldspars", so designated by the analytical software. By comparison, four Tuff IA sub-beds and an un-named tuff immediately above it are associated with "entering saline / alkaline" periods (or all in one climatic period) over a short four thousand year-span. The next tuff-fall was about 18 ky later, when Berry's data show the system going beyond a strong concentration dry (saline /alkaline) peak all the way to a wet (dilute) peak.

The lack of regularity and an inversion of the expected chemistry suggest that unexplained mechanisms were operating from 1.920 Ma throughout Bed 1 deposition. XRD results do not seem to support a relationship between current mineralogy and climate cycles.

4.2.3 Authigenesis

Here, plots of selected oxides explore relationships between the oxides and timing of their strongest appearances in the XRF-age record.

4.2.3.1 Authigenic Phillipsite and Sanidine Climate Cycle Proxies

Phillipsite and sanidine appear so randomly in the tuffs that they are not effective mineral indicators of Milankovitch precession and obliquity-type climate cycles as identified by Berry (2012). If there is cyclicity embedded in the alternation of mineral occurrences, it is on the order of 9 to <1 ky and highly variable. These increments could accommodate one to six Bond Cycles (Bond et al., 1997). Hay's 1963 discussions of syntheses of phillipsite and chabazite all involved

quite strong (minimum 5000 mg/l) saline / alkaline solutions. If that minimum test (5000 mg/l) was likely representative of wet-lake, dilute times, then it is not surprising that phillipsite is found at "dilute" water cycle peaks. (More probably there are other factors at work, such as influences of varying biogenic processes and changing groundwater flow (vertical, horizontal, and lateral) and composition.

The mineral dichotomy on either side of the age gap is possibly explained by the climate being generally wetter for the entire 51 Ky before 1.869 Ma and the basin and groundwater exhibiting relatively freshwater-like chemistry during and long after sediment deposition. The prevalence of Ca and Mg minerals suggests this and that the more mobile cations expected from volcanic rocks were removed by flushing. If a generally drier period then ensued for the remaining 57 Ky of Bed I deposition after 1.857 Ma, the expected saline / alkaline lake authigenic environment could have prevailed. This could lead to two possible conclusions: tuffs below the 1.869 Ma mark were formed then preserved from "contamination" in immobile fresh groundwater until incision drained the whole aquifer, or the area was subject to essentially one long cycle of one wet and one dry half-cycles of authigenesis. Both conclusions would be in accord with Mees et al. (2005) to the effect that early Bed I was subjected to less concentrated water than the latter half.

4.2.3.2 Ammonium Phillipsite

Because natural ammonium-rich phillipsites exist in other places (Dwairi, I.M., 1998; and Öprinar, 2008), it would not be surprising to find them at Olduvai Gorge. However, comparison of XRD cards for phillipsite (NH₄) and phillipsite (Na) reveal very similar peaks; therefore, one cannot accept the presence of ammonium phillipsite without further analysis. Volcanic emissions, because ammonia is minor, uncommon, and easily air-dispersed, are a very unlikely

origin for such large quantities and over such long time spans. Ammonium, K, and Na are close to each other in cation exchange capacity selectivity for phillipsite, which makes repeated exchanges possible. Non-ammonia phillipsites might be indicators of stratigraphic levels and times of low bioactivity (and inhospitable habitat for hominin society), if it could be determined that sediments deposited at different times were not confounded with each other by groundwater chemistry and movement changing through time. Analcime, an Na silicate here associated with Ca and Mg minerals, is not associated with phillipsite. Zeolitization seems to prefer low CaO/MgO, but it is age that clearly correlates with phillipsite occurrence in Bed I tuffs.

4.2.3.3 Suite of Zeolites

The suite of prominent zeolites actually identified from Bed I tuffs was small (phillipsite-NH₄, phillipsite-Mg and analcime) compared to the seven reported by Hay (1963, 1964, 1970, and 1976) and Larsen (2008). Perhaps the XRD analyses and data processing were insufficiently aggressive.

4.2.4 *Cation Oxide Comparisons*

Figure 13 with (Na₂O + K₂O) wt.%s plotted against CaO%/MgO wt.%s reveals two basic, but overlapping fields, one for the phillipsite tuffs (1.857 Ma or younger) and one for non-phillipsite tuffs (1.869 Ma or older). That gap contained no tuff-falls. Figure 14 puts MgO in the denominator on both axes. If anything the scatter is greater, but the two fields persist. This method removed Mg from the respective systems.

Three-component plotting Figure 15 exposes the composition split more dramatically than in simpler x-y charts. Hand-picked "clean glass" and tephra samples, included for comparison, demonstrate high alkali metal content (McHenry, 2005; McHenry, 2009). Because time is not a plotted variable, it is quite clear there is a difference in tuff composition that goes

beyond considerations of time and a listing of named major minerals. The phillipsite field is defined to be above the 50% (Na₂O +K₂O) line, except for the upper elevation Tuff IE, GA-L-52-99, at 24.53 m, 1.831 Ma. That corresponds to a dilution peak on Figure 7 (Berry, 2012). Thirty percent MgO is another dividing line. Non-phillipsite tuff sample GA-L-151-99 is alone and surrounded by phillipsite tuffs. It contains 74% alkalis and is not phillipsite but reported as "f-spar, sanidine-like" without an accompanying second-ranking mineral of consequence. It is apparently all authigenic feldspar. According to Berry's (2012) data, it formed at or just after a dry-period, saline / alkaline peak condition. It is the lowermost Tuff IF sample.

Cation frequency map, Figure 16 shows a number of interesting relationships, but the large question arising, when taken with the 1.869-1.857 Ma gap seen in other data, is: Why did Ca become so prominent in volcanic deposits then almost disappear from later tuffs? A secondary question is: What caused the short Ca return at 1.831 Ma? Na and K are noted to be ubiquitous, bound in phillipsite and K-feldspars or available for reactions, depending on pH, Eh, T, salinity, and other variables, such as groundwater flux. Ca is certainly dominant in the early tuffs but inexplicably appears again as a major element twice in later times. Na and K are significant in all but one tuff, even those high in Ca. Analcime is an Na silicate, yet it is associated with significant Ca presence on both occasions. Many anomalies exist.

Plotting tuff age against CaO/MgO wt.% only (Figure 17) and separately for phillipsite, analcime, and non-zeolite tuffs again supports the visual impression from Table 5 that two different populations exist.

Tuff age plotted against Al₂O₃ Wt. % / MgO Wt.% (Figure 18) suggested that Al was the missing element for zeolitization to occur above a ratio of 3.00. Phillipsite can use Mg for cation

exchange, but does not need it for authigenesis. Cycles did not appear in this analysis but group separation is very clear, again.

4.2.5 *Tuff Color Analysis*

Before oxides were plotted in a search for possible relationships between variables, Munsell Soil Color Chart readings (Table 6) had revealed a change from lighter to darker shades. It was not sharp but focused attention on the gap from 1.869 Ma to 1.857 Ma. This matched recognition that phillipsite content in tuffs began with 1.857 Ma.

4.2.6 *Unanticipated Findings*

4.2.6.1 1.869-1.857 Ma Authigenesis Transition

Multiple ways of examining tuff samples' characteristics point to a radical change in mineralogy before or at 1.857 Ma, but do not explain the reasons. Silicon (the most abundant cation) and aluminum (a close second) are the statistically significant two of six common cations in samples, with respect to time correlation, for the period after 1.857 Ma compared to those for prior times. No oxides of Ca, K, Na, or Mg were significantly correlated with change of age to help explain the mineralogy split. The importance of Si and Al matches the finding from Figure 15. With allowance for slightly differing age models, Hay and Kyser's (2001, their Figure 10) finding of modestly above geological average lake water concentration from 1.924 Ma to 1.863 Ma covers the early period before phillipsite is seen beginning at 1.857 Ma. However, sanidine and other high-K minerals did exhibit some prominence earlier among tuffs from 1.891 through 1.869 Ma.

Taken together, those findings raise two questions: 1) Why are there no K-feldspars seen until 1.891 Ma; and 2) Why would any / all early zeolite undergo secondary authigenesis to K-feldspars from 1.891 through 1.869 Ma then experience only sporadic secondary authigenesis to

K-feldspars from 1.857 onward through 1.803 Ma?

The lake margin findings of Mees et al. (1997) suggest a combination of changes through time. First, deposition into relatively dilute saline / alkaline waters produced analcime. Second, pore water replacement by higher Na/K waters resulted in chabazite and other zeolite formation. Eventually, high K, Na, Al, and Si waters supported authigenesis of such minerals as K-spars and phillipsite. Mees et al. further propose that the transition was a relatively abrupt undefined depositional environment event. That contention appears to match findings of this study, but the timing cannot be matched, because their work began with Tuff IB - just above the time / composition break found in this study. Mees et al.'s (2005) work on lake margin authigenesis and remarks that zeolites form most readily in subaerial (take that as aerobic) contexts might suggest that the times after 1.857 Ma found the Bed I paleolake in a situation of frequently changing rapid transgression and regression. The entire lake could have been essentially cycling between shallow lake, margin, and playa with conditions easy for zeolites to quickly evolve through the sequence of analcime and chabazite to other zeolites, like phillipsite, and K-feldspars.

4.2.6.2 Potential Micro-cycles

Alternations of phillipsite and K-spar authigenesis could be explained by thus far unrecognized phenomena. Deocampo (2004a) suggested the possibility of unidentified factors, like "paleohydrologic balance" shifts, such as changes in the ratio of precipitation to evaporation rates, not only tectonic changes. These demonstrations of varied outcomes from supposedly chemically similar or identical original minerals and waters support his hypothesis.

4.2.6.3 Groundwater

Stollhofen and Stanistreet (2012) raised the question of what happened to groundwater when the incising gorge drained the lake. While that was 1.4 My after the switch from a

predominantly Ca-rich to K-rich mineralization, it or prior geological "step functions", like fault movements, might have radically changed how, what, and how long given waters were stored and moved through regional and local Bed I aquifers beneath the CB, in both un-incised and incised states.

4.3 Paleo-environmental Implications

No clear support for climatic cycles is evident in these findings to match Berry's four. This divergence from Berry's conclusions is shown but not yet explained. Berry's findings, while not confirmed, are not rejected, because the overlapping sample populations were intentionally, significantly different. If there is evidence for cycles, it is for lesser changes most likely arising from short-term climate or tectonic sources, as suggested by Deocampo (2004a). It is also likely that tuff alteration is not itself a sensitive enough proxy to document paleoenvironmental changes through time, to the same degree that clay geochemistry does. Holocene climate 1500 yr Bond Cycles (Bond et al., 1999) was validated by Gupta et al. (2003) as driving cyclicality of southwestern Indian Ocean Monsoons. Those monsoons similarly have been shown to impact East African climate (Ashley et al. citing Nicholson (1996), 2014; and Trauth et al., 2007). As a result, it is not unreasonable to speculate that such short-term cycles also might have operated in the early Pleistocene. They could have influenced Olduvai Gorge's climate and caused short cycles in climate and in a seemingly chaotic pattern of alternating phillipsite and K-feldspar authigenesis from 1.857 to 1.803 Ma. The radical 1.869-1.857 Ma chemistry change might reflect a significant change in environmental conditions, but clues to its nature and cause were not discovered.

4.4 Future Work

To be redundant with other's writings, much more work remains to generate increasingly accurate and precise age measurements. It is not in the scope of this study to do more than to note that a revisit to some specifics of wet / dry cycle conclusions drawn in Ashley's and others' papers might be in order to recheck habitat environment conditions vs. time. The 1.845 Ma (Blumenshine et al., 2003) age remains essentially valid, but earlier literature needs to be reviewed and updated from models using 1.79 Ma for the age of Tuff IF in light of Deino's new 1.803 Ma age. That represents more than half of one 21 ky precessional cycle and could significantly modify climate / precession / habitat correlations based on age rather than sample depth. It became clear in the process of this study that ever more accurate and precise radiometric ages are needed to establish a fully trustworthy basis for all other research that has a time component. This is true not only for current anchor dates but to bridge the gaps between them, especially if beds overlying Bed I have equally problematic situations.

If deemed worth the effort, the tuff XRD files could be reprocessed more aggressively in search of additional zeolites and other minerals and to quantify mineral content for more detailed comparison with XRF elemental data. At least a few samples should be chemically checked to determine whether and how much NH_4 is present in the phillipsite. If present, the degree of NH_4 exchange completion could potentially give clues to past groundwater quality, especially if compared from bottom to top of the entire Paleolake Olduvai CB. Include investigating presence / absence of phillipsite ammonium as a signal of habitat bioactivity at specific times and possibly reflective of water conditions suitable for sustaining complex life.

Lack of regularity and the inversions of expected chemistry (high frequency of phillipsite and sanidines produced in presumably relatively dilute conditions) suggest that closer scrutiny of

mineralogy is needed to unearth unexplained processes or events operating from 1.920 Ma throughout Bed 1 deposition. What changed the alkaline earth domination of early Bed I tuffs to a predominantly alkali domination from then on? Those influences on mineralogy long after the respective tuff sediment depositions could be biological, chemical, or tectonic.

Evidence of Bond Cycles should be sought through stricter statistical analysis and such techniques as carbon, deuterium/hydrogen, and oxygen isotope determinations in minerals and organic residues. Isotope analyses might be accomplished by the simple means of revisiting data from past work, but focused on the idea of the possibility of short cycles.

Non-tuff deposits should be further investigated to find whether the 1.869-1.857 Ma chemical discontinuity would be further substantiated and reveal why local habitats became more attractive to hominins, as shown by fossil discoveries from 1.857 Ma onward. And, Berry's (2012) XRF data for non-tuffs only (setting the tuff data aside) should be re-analyzed to determine if the identified cycles might acquire better definition after elimination of the seemingly discrepant tuff results of this study.

5. CONCLUSIONS

5.1 Age model

The new model developed for this study worked very well for these sediments, and the anchor dates and sedimentation factors from Deino (2012) with minor amendments are recommended for further use until yet better anchor dates become available. Prior models using 1.79 Ma for the age of Tuff IF should be reviewed in light of Deino's new age of 1.803. One half of one 21 ky precessional cycle is too large an increment to disregard.

5.2 Mineralogy

XRD results do not support the hypothesis of a positive relationship between current mineralogy and climate cycles. There could have been other, subtle influences. Phillipsite and sanidine appear so randomly in the tuffs that they seem useless for whole-mineral indicators of Milankovitch precession and obliquity-type climate cycles identified by Berry (2012). If cyclicity is embedded in the alternation of mineral occurrences, it is on the order of 9 to <1 ky and highly variable. More probably there are other factors at work, such as influences of varying biogenic processes and changing groundwater flow (vertical vs. horizontal and direction) and composition.

5.3 1.869-1.857 Ma Authigenesis

A major change in mineralogical and/or chemical regime related to protolith or water composition probably occurred between 1.869 and 1.857 Ma. The early period up to 1.869 Ma was characterized by prominence of Ca-rich and Mg-rich minerals, and the later period by K-rich minerals (Table 5). However, there was no exclusivity; Ca, Mg, Na, and K minerals were found as second rank, if not first rank in both periods.

Considering the CaO / MgO ratio as a weathering index, Figures 13 and 14 suggest that, in general, the older time increment experienced stronger weathering than the younger. But, there are overlaps and no obvious indications as to why there was such a sharp authigenic age break in shifting from mostly Ca, Mg, and K minerals to phillipsites. What kept the older period sanidines and other K-feldspars from reacting to form phillipsites in presumably dilute waters, when they did so during the younger period? Shortage of Al appears to be a controlling factor in the period 1.869 Ma and earlier (Figure 18). This agrees with the literature on zeolite authigenesis.

Contrary to accepted research and theory, study results do not show a co-relation between zeolite authigenesis and necessity for saline / alkaline water. In fact, phillipsite, the one prominent zeolite in the tuffs, occurs more times in tuffs associated with wet-period "dilute" lake waters than in supposed dry-period waters. Zeolitization seemed to prefer a low CaO/MgO regime, but it is age that sharply and consistently correlates in this study.

Phillipsite authigenesis might have included incorporation of NH_4 , whether initially or in a later modification. This finding is inconclusive, however, pending a determination that NH_4 is the exchanged ion in the phillipsites. If present, the NH_4 could be an indicator of high levels of bioactivity in and around the lake capable of supporting the demanding needs of hominins and worthy of further examination; or, it could merely signal salt tolerant microorganism growths, such as seen in modern salt lakes.

REFERENCES

- Agresti, A., 1997, An introduction to categorical data analysis, New York, John Wiley and Sons, 290 p.
- Ashley, G.M., 2007, Orbital rhythms, monsoons, and playa lake response, Olduvai Basin, Equatorial East Africa, ca. 1.85–1.74 Ma: *Geology*, v. (35), p. 1091-1094.
- Ashley, G.M., Undated, Photocopy of typed sample number / depth tabulation for 1999 Olduvai stratigraphic column: provided to Berry, 2011 and received from P. Berry, 2012, 4 p.
- Ashley, G. M., Barboni, D., Dominguez-Rodrigo, M., Bunn, H.T., Mabulla, A.Z.P., Diez-Martin, F., Barba, R., and Baquedano, E., 2010a, Paleoenvironmental and paleoecological reconstruction of a freshwater oasis in savannah grassland at FLK North, Olduvai Gorge, Tanzania: *Quaternary Research*, v. 74, p. 333–343.
- Ashley, G.M., Dominguez-Rodrigo, M., Bunn, H.T., Abulla, A.Z.P, and Baquedano, E., 2010b, Sedimentary geology and human origins: A fresh look at Olduvai Gorge, Tanzania: *Journal of Sedimentary Research*, Vol. 80 (8), p. 703-709.
- Ashley, G.M., Hay, R.L., Renaut, R.W., and Mollel, G.F., 1999, Photocopy of unpublished, annotated Olduvai Gorge Locality 80 Bed I field note stratigraphic column: 14 July, 9 p.
- Baker, B.H., 1986, Tectonics and volcanism of the southern Kenya Rift Valley and its influence on rift sedimentation: Sedimentation in the African Rifts: in Frostick, et al., eds., Special Publication Vol. 25, The Geological Society of London, p. 45–57.
- Bates, R.L. and Jackson, J.A., 1984, Dictionary of geological terms: 3rd Ed., American Geological Institute, New York, Anchor Books, 571 p.
- Baur, W. H., Fischer, R. X., PHI: Fischer, R.X., Baur, W.H. (ed.). SpringerMaterials - The Landolt-Börnstein Database: http://www.springermaterials.com/docs/info/978-3-540-45870-8_36.html (accessed February 2014)
- Berry, P.A., 2012, Lake cycles and sediments: Locality 80, Olduvai Gorge, Tanzania (M.S thesis): Geosciences paper 47, Georgia State University, Atlanta, Georgia, 63 p.
- Berry, P.A., 2014, Personal communication, Climate cycle graph construction process.
- Blumenschine, R.J., Peters, C.R., Masao, F.T., Clarke, R.J., Deino, A.L., Hay, R.L., Swisher, C.C., Stanistreet, I.G., Ashley, G.M., McHenry, L.J., Sikes, N.E., van der Merwe, N.J., Tactikos, J.C., Cushing, A.E., Deocampo, D.M., Njau, J.K., and Ebert, J.I., 2003, Late Pliocene homo and hominid land use from western Olduvai Gorge, Tanzania: *Science*, v. 299, p. 1217–1221.
- Boggs, S., 2012, Principles of sedimentology and stratigraphy: 5th Ed., Upper Saddle River, New Jersey, Pearson Prentice-Hall, 585 p.
- Bond, G., Showers, W., Cheseby, M., Lotti, R., Almasi, P., deMenocal, P., Priore, P., Cullen, H., Hajdas, I., Bonani, G., 1997, *Science*, Vol. 278 (5341), p. 1257-1266.
- Cerling, T.E., and Hay, R.L. (1986), An isotopic study of paleosol carbonates from Olduvai Gorge, *Quaternary Research*, Vol. 25, No. 1, p. 63-78.
- Coto, B., Martos, C., Peña, J.L., Rodriguez, R., and Pastor, G., 2012, Effects in the solubility of CaCO₃: Experimental study and model description: *Fluid Phase Equilibria*, v. 324, p. 1-7: <http://eciencia.urjc.es/bitstream/10115/6052/1/REPOSITORIO%20ANGEL.pdf> (accessed November 2013)
- Dawson, J.B., 2008, The Gregory rift valley and Neogene-recent volcanoes of northern Tanzania: *Memoir No. 33*, The Geological Society of London, 112 p.

- Deino, A., 2012, $^{40}\text{Ar}/^{39}\text{Ar}$ dating of Bed I, Olduvai Gorge, Tanzania, and the chronology of early Pleistocene climate change: *Journal of Human Evolution*, v. 63, p. 251-273.
- Deino, A., 2013, Personal email communication: Request for interpretation of $^{40}\text{Ar}/^{39}\text{Ar}$ dating of Tuff Bed I.
- deMenocal, P.B., 1995, Plio-Pleistocene African climate: *Science*, v. 270, (5233), p. 53-59.
- Deocampo, D.M., 2004a, Authigenic clays in East Africa: Regional trends and paleolimnology at the Plio-Pleistocene boundary, Olduvai Gorge, Tanzania: Rapid communication, *Journal of Paleolimnology*, v. 31 (1), p. 1-9.
- Deocampo, D.M., 2004b, Hydrogeochemistry in the Ngorongoro Crater, Tanzania, and implications for land use in a World Heritage Site: *Applied Geochemistry*, v. 19 (5), p. 755-767.
- Deocampo D.M., and Jones B.F. (2014), *Geochemistry of Saline Lakes*. In: Holland H.D. and Turekian K.K. (eds.), *Treatise on Geochemistry*, Second Edition, Vol. 7, Elsevier, Oxford, p. 437-469.
- Dwairi, I.M., 1998, Evaluations of Jordanian zeolite tuff as a controlled slow-release fertilizer for NH_4^+ : Research Article, *Environmental Geology*, v. 34 (1), p. 1-4.
- Eugster, H.P. and Jones, B.F., 1979, Behavior of major solutes during closed-basin brine evolution: *American Journal of Science*, v. 279 (6), p. 609-631.
- Google Earth, 2014, Olduvai Gorge, Tanzania, Satellite photography with dynamic coordinates (accessed January 2014)
- Graham, D. and Midgley, N., 2006, Triangular diagram plotting spreadsheet: TRI-PLOT, Version 1-4-2-3, Loughborough University, UK:
http://www.google.com/url?sa=t&rct=j&q=&esrc=s&source=web&cd=3&ved=0CDQQFjAC&url=http%3A%2F%2Fwww-staff.lboro.ac.uk%2F~gydjg2%2Fdownloads%2Ftri-plot_v142.xls&ei=wY8KU4yxJtKLkAe1jYGoBA&usq=AFQjCNGNTIqt4yo8xxshoxPofv3H8PtTLg&bvm=bv.61725948,d.eW0 (accessed the 2006 update, February 2014)
- Gupta, A.K. 2003, Abrupt changes in the Asian southwest monsoon during the Holocene and their links to the North Atlantic Ocean, *Nature*, Vol. 421 (6921), p. 354-357.
- Hay, R.L., 1963, Zeolite weathering in Olduvai Gorge, Tanganyika: *Geological Society of America Bulletin*, Vol. 74, p. 1281-1286.
- Hay, R.L., 1964, Phillipsite of saline lakes and soils, *American Mineralogist*: v.49, p. 1366-1387.
- Hay, R.L., 1970, Silicate reactions of three lithofacies of a semi-arid basin, Olduvai Gorge, Tanzania, Special Paper 3, *Mineralogical Society of America*, p. 237-255.
- Hay, R. L., 1976, *The geology of Olduvai Gorge: A study of sedimentation in a semiarid basin*, Berkeley, University of California Press, 203 p.
- Hay, R.L. and Kyser, T.K., 2001, Chemical sedimentology and paleoenvironmental history of Lake Olduvai a Pliocene lake in northern Tanzania: *Geological Society of America Bulletin*, v. 113 (12), p. 1505-1521.
- Holdship, S.A., 1976, The paleolimnology of Lake Manyara, Tanzania: A diatom analysis of a 56 meter sediment core, (Ph.D. thesis): Duke University, 133 p.
- IBM Corporation, 2010, *IBM SPSS Statistics for Windows*, Version 19.0. Armonk, NY: IBM Corporation.
- Jakkula, 2005, Synthesis of zeolites and their application as soil amendments to increase crop yield and potentially act as controlled release fertilizers (Ph.D. thesis): University of Wolverhampton, U.K., 273 p.

- Jones, B.F., Eugster, H.P., and Rettig, S.L., 1977, Hydrochemistry of Lake Magadi basin, Kenya: Abstract, *Geochimica et Cosmochimica*, v. 47 (1), p. 53-72.
- The Laetoli-Olduvai Field School: <http://www.olduvaiproject.org/the-laetoli-olduvai-field-school/> (accessed February 2014)
- Larsen, D., 2008, Revisiting silicate authigenesis in the Pliocene–Pleistocene Lake Tecopa beds, southeastern California: Depositional and hydrological controls: *Geosphere*, v. 4 (3), p. 000–000; doi: 10.1130/GES000152.1.
- Leakey, M.D., Hay, R.L., Thurber, D.L., Protsch, R., and Berger, R., 1972, Stratigraphy, archaeology, and age of the Ndotu and Naisiusiu Beds, Olduvai Gorge, Tanzania: *World Archaeology*, v. 3 (3), p. 328-341.
- Lee, J., 2010, updated 2012, Milankovitch cycles: in *The Encyclopedia of Earth*, Boston University: <http://www.eoearth.org/view/article/154612/> (accessed (February 2014)
- Magill, C.R., Ashley, G.M., and Freeman, K.H., 2012a, Ecosystem variability and early human habitats in eastern Africa: *Proceedings of the National Academy of Sciences*, v. 110 (4), p. 1167-1175.
- Magill, C.R., Ashley, G.M., and Freeman, K.H., 2012b, Water, plants, and early human habitats: *Proceedings of the National Academy of Sciences*, v. 110 (4), p. 1175-1180.
- McHenry, L.J., 2005, Phenocryst composition as a tool for correlating fresh and altered tephra: Bed I, Olduvai Gorge, Tanzania, *Stratigraphy*, v. 2 (2), p. 101–115.
- McHenry, L.J., 2009, Element mobility during zeolitic and argillic alteration of volcanic ash in a closed-basin lacustrine environment: Case study Olduvai Gorge, Tanzania: *Chemical Geology*, v. 265, p. 540–552.
- Mees, F., Stoops, G., Van Ranst, E., Paepe, R., and Van Overloop, E., 2005, The nature of zeolite occurrences in deposits of the Olduvai Basin, Northern Tanzania, *Clay and Clay Minerals*, Vol. 53 (6), p. 659-673.
- Miller, C.D., 1989, Potential hazards from future volcanic eruptions in California, U.S. *Geological Survey Bulletin* 1847, 17 p.
- Munsell Color Xrite, 2009 Revision, Munsell soil color charts: 2012 production, Looseleaf, Grand Rapids, Michigan. Munsell Color, 13 charts.
- Ngorongoro Conservation Area Authority, NCAA: <http://www.ngorongorocrater.org/oldupai.html> (accessed February 2014)
- Özpinar, Y., 2008, The mineralogic, petrographic and ion exchange capacity features of tuffs containing chabazite and phillipsite minerals in Sandikli, Afyon Region and their usage in agriculture, Southwest Anatolia, Turkey: *Mineral Research & Exploration Bulletin*, v. 137, p. 29-48.
- PANalytical B.V. (2011), Data Viewer, Almedo, Netherlands.
- PANalytical B.V. (2011), Data Collector, ver. 4.1.0.25, Almedo, Netherlands.
- Potts, R. (2013), Hominin evolution in settings of strong environmental variability, *Quaternary Science Reviews*, Vol. 73, p. 1-13.
- Robinson, D. and Leake, B.E., 1975, Sedimentary and igneous trends on AFM diagrams: *Geological Magazine*, v. 112 (3), p. 305-307.
- Schaetzl, R.J., 2005 corrected 2007, *Soils: Genesis and geomorphology*, Cambridge University Press, United Kingdom, 817 p.
- Sheppard, R.A. and Gude, A.J., 1968, Distribution and genesis of authigenic silicate minerals in tuffs of Pleistocene Lake Tecopa, Inyo County, California: U.S. Geological Survey Professional Paper 597, 38 p.

- Sinclair, A.R.E., Packer, C., Mduma, S.A.R., and Fryxell, M., 2009, Serengeti III: Human impacts on ecosystem dynamics: Chicago, University of Chicago Press, 522 p.
- Sikes, N.E. and Ashley, G.M., 2007, Stable isotopes of pedogenic carbonates as indicators of paleoecology in the Plio-Pleistocene, upper Bed I, western margin of the Olduvai Basin, Tanzania: *Journal of Human Evolution*, v. 53, p. 574-594.
- SPSS Version 19 (2010)
- Stollhofen, H. and Stanistreet, I.G., 2012, Plio-Pleistocene synsedimentary fault compartments, foundation for the eastern Olduvai Basin paleoenvironmental mosaic, Tanzania: *Journal of Human Evolution*, v. 63, p. 309-327.
- Zimmermann, K.A., 2013, Olduvai Gorge: Oldest Evidence of Mankind's Evolution: LiveScience: <http://www.livescience.com/40455-olduvai-gorge.html> (accessed Feb 2014)

APPENDICES

Appendix A Berry (2012) XRF oxide data for Bed I Tuffs and selected ratios for two time intervals

Sample ID	Depth from Bottom	Elements Present in Weight Percent: Raw Data										Total Wt. %
		SiO ₂	TiO ₂	Al ₂ O ₃	Fe ₂ O ₃	MnO	MgO	CaO	Na ₂ O	K ₂ O	P ₂ O ₅	
GA-L-X-99	Meters											%
153	27.40	53.05	0.84	13.12	6.92	0.09	2.51	4.85	4.19	5.54	0.12	91.23
151	27.15	60.43	0.66	15.82	5.23	0.09	1.80	2.57	3.17	9.07	0.10	98.94
52	24.53	55.77	0.80	12.42	4.94	0.10	2.30	11.11	3.53	5.87	0.16	97.00
53	24.28	50.85	1.25	9.54	4.25	0.15	7.68	7.06	2.72	7.85	0.13	91.48
54	24.24	55.33	0.65	16.61	6.12	0.03	0.90	1.46	5.47	6.63	0.07	93.27
57	24.00	53.56	0.90	13.22	8.66	0.10	4.22	3.00	3.96	6.15	0.15	93.92
61	24.30	54.86	0.78	13.24	6.37	0.13	4.71	2.06	4.34	5.71	0.14	92.34
64	22.71	51.86	0.85	11.24	6.21	0.12	5.19	5.12	2.63	7.39	0.13	90.74
67	21.87	56.43	0.73	14.53	5.86	0.04	1.88	0.83	4.87	6.27	0.07	91.51
145	19.60	62.06	0.82	16.00	4.08	0.03	1.49	0.62	5.89	6.66	0.05	97.7
104	16.70	48.69	0.30	11.63	4.25	0.08	2.91	11.49	3.75	5.86	0.08	89.04
100	16.05	47.46	0.89	9.05	8.05	0.18	6.75	8.52	1.91	6.52	0.13	89.46
97	15.82	50.13	0.65	11.07	6.51	0.16	4.37	5.59	2.92	6.61	0.11	88.12
95	15.56	54.44	0.45	13.17	5.69	0.09	2.87	5.85	3.24	7.39	0.14	93.33
92	15.09	35.90	0.91	7.32	8.99	0.07	4.45	12.69	1.75	5.46	0.09	77.63
85	14.20	45.15	0.49	11.55	8.66	0.08	4.98	9.51	2.78	6.84	0.12	90.16
128	11.40	40.83	0.64	9.02	11.06	0.07	3.46	6.91	2.92	6.06	0.16	81.13
126	11.11	46.38	0.77	10.08	7.44	0.10	4.72	6.49	2.89	7.55	0.18	86.6
124	10.74	16.52	0.25	2.30	7.67	0.04	2.90	26.50	1.74	1.70	0.06	59.68
117	9.45	37.09	0.78	6.41	5.77	0.09	6.38	11.43	2.46	4.54	0.14	75.09
24	4.95	22.98	0.41	2.63	1.99	0.07	21.04	15.87	3.53	2.01	0.06	70.59
19	3.83	38.18	0.87	6.99	5.32	0.07	9.01	15.43	2.32	3.65	0.15	81.99
18	3.60	36.73	0.76	7.85	5.90	0.12	13.11	10.27	4.56	2.32	0.05	81.67
17	3.40	38.50	1.19	8.41	6.25	0.12	10.15	13.52	3.48	2.83	0.08	84.53
16	3.20	33.73	0.78	7.69	5.59	0.12	8.16	19.21	2.64	2.99	0.16	81.07

Normalized Data, wt. %										
SiO ₂	TiO ₂	Al ₂ O ₃	Fe ₂ O ₃	MnO	MgO	CaO	Na ₂ O	K ₂ O	P ₂ O ₅	Total
58.15	0.92	14.38	7.59	0.10	2.75	5.32	4.59	6.07	0.13	100.00
61.08	0.67	15.99	5.29	0.09	1.82	2.60	3.20	9.17	0.10	100.00
57.49	0.82	12.80	5.09	0.10	2.37	11.45	3.64	6.05	0.16	100.00
55.59	1.37	10.43	4.65	0.16	8.40	7.72	2.97	8.58	0.14	100.00
59.32	0.70	17.81	6.56	0.03	0.96	1.57	5.86	7.11	0.08	100.00
57.03	0.96	14.08	9.22	0.11	4.49	3.19	4.22	6.55	0.16	100.00
59.41	0.84	14.34	6.90	0.14	5.10	2.23	4.70	6.18	0.15	100.00
57.15	0.94	12.39	6.84	0.13	5.72	5.64	2.90	8.14	0.14	100.00
61.67	0.80	15.88	6.40	0.04	2.05	0.91	5.32	6.85	0.08	100.00
63.52	0.84	16.38	4.18	0.03	1.53	0.63	6.03	6.82	0.05	100.00
54.68	0.34	13.06	4.77	0.09	3.27	12.90	4.21	6.58	0.09	100.00
53.05	0.99	10.12	9.00	0.20	7.55	9.52	2.14	7.29	0.15	100.00
56.89	0.74	12.56	7.39	0.18	4.96	6.34	3.31	7.50	0.12	100.00
58.33	0.48	14.11	6.10	0.10	3.08	6.27	3.47	7.92	0.15	100.00
46.25	1.17	9.43	11.58	0.09	5.73	16.35	2.25	7.03	0.12	100.00
50.08	0.54	12.81	9.61	0.09	5.52	10.55	3.08	7.59	0.13	100.00
50.33	0.79	11.12	13.63	0.09	4.26	8.52	3.60	7.47	0.20	100.00
53.56	0.89	11.64	8.59	0.12	5.45	7.49	3.34	8.72	0.21	100.00
27.68	0.42	3.85	12.85	0.07	4.86	44.40	2.92	2.85	0.10	100.00
49.39	1.04	8.54	7.68	0.12	8.50	15.22	3.28	6.05	0.19	100.00
32.55	0.58	3.73	2.82	0.10	29.81	22.48	5.00	2.85	0.08	100.00
46.57	1.06	8.53	6.49	0.09	10.99	18.82	2.83	4.45	0.18	100.00
44.97	0.93	9.61	7.22	0.15	16.05	12.57	5.58	2.84	0.06	100.00
45.55	1.41	9.95	7.39	0.14	12.01	15.99	4.12	3.35	0.09	100.00
41.61	0.96	9.49	6.90	0.15	10.07	23.70	3.26	3.69	0.20	100.00

Appendix B Minerals cited in Olduvai Gorge literature

MINERAL	NOTES		EMPIRICAL FORMULAE	ONLINE RESOURCES (Active links)
Augite	Beds I-B, I-D, & IF	Hay (1976)	$\text{Ca}_{0.9}\text{Na}_{0.1}\text{Mg}_{0.9}\text{Fe}^{2+}_{0.2}\text{Al}_{0.4}\text{Ti}_{0.1}\text{Si}_{1.9}\text{O}_6$	http://webmineral.com/data/Augite.shtml
sodic augite	5-10% lower Bed II sandstones	Hay (1976)	$\text{Na}_2\text{CaMg}_3\text{Fe}^{2+}_2(\text{Si}_8\text{O}_{22})(\text{OH})_2$	http://webmineral.com/data/Richterite.shtml
CaCO_3 authigenic	euhedral	Hay (1976)	CaCO_3	
calcite authigenic	5-10% Bed I claystones	Hay (1976)	CaCO_3	
calcium carbonate authigenic	micrite		CaCO_{3f}	
celadonite		Hover & Ashley (2003)	$\text{KMg}_{0.8}\text{Fe}^{2+}_{0.2}\text{Fe}^{3+}_{0.9}\text{Al}_{0.1}\text{Si}_4\text{O}_{10}(\text{OH})_2$ *In celadonite-rich, waxy claystone	http://webmineral.com/data/Celadonite.shtml - .UfVCcIOhUrA http://www.mindat.org/min-926.html
Clays authigenic		Hay & Kyser (2013)		
illite			$\text{K}_{0.6}(\text{H}_3\text{O})_{0.4}\text{Al}_{1.3}\text{Mg}_{0.3}\text{Fe}^{2+}_{0.1}\text{Si}_{3.5}\text{O}_{10}(\text{OH})_2 \cdot (\text{H}_2\text{O})$	http://webmineral.com/data/Illite.shtml
illite/smectite		Hay & Kyser (2001)		
motmorillonite			$\text{Na}_{0.2}\text{Ca}_{0.1}\text{Al}_2\text{Si}_4\text{O}_{10}(\text{OH})_2(\text{H}_2\text{O})_{10}$	http://webmineral.com/data/Montmorillonite.shtml
Smectite		Hay & Kyser (2001)		
Dawsonite			$\text{NaAl}(\text{CO}_3)(\text{OH})_2$	http://webmineral.com/data/Dawsonite.shtml
Dolomite			$\text{CaMg}(\text{CO}_3)_2$	http://webmineral.com/data/Dolomite.shtml
Feldspars				
andesine	Dominant in Bed I		$\text{Na}_{0.6}\text{Ca}_{0.4}\text{Al}_{1.4}\text{Si}_{2.6}\text{O}_8$	http://webmineral.com/data/Andesine.shtml
anorthoclase	Beds I-B, I-D, & I-F	Hay (1976)	$\text{Na}_{0.75}\text{K}_{0.25}\text{AlSi}_3\text{O}_8$	http://webmineral.com/data/Anorthoclase.shtml
K-feldspar - authigenic			microcline: KAlSi_3O_8 intermediate sanidine: $\text{K}_{0.75}\text{Na}_{0.25}\text{AlSi}_3\text{O}_8$	http://webmineral.com/data/Microcline.shtml http://webmineral.com/data/Sanidine.shtml
labradorite	Dominant in Bed I w/andesite		$\text{Na}_{0.4}\text{Ca}_{0.6}\text{Al}_{1.6}\text{Si}_{2.4}\text{O}_8$	http://webmineral.com/data/Labradorite.shtml
oligoclase		Hay (1976)	$\text{Na}_{0.8}\text{Ca}_{0.2}\text{Al}_{1.2}\text{Si}_{2.8}\text{O}_8$	http://webmineral.com/data/Oligoclase.shtml
Fluorite	50% of Bed II claystones		CaF_2	http://webmineral.com/data/Fluorite.shtml
Hornblende		Hay (1976)	magnesio-hornblende: $\text{Ca}_2\text{Mg}_4\text{Al}_{0.75}\text{Fe}^{3+}_{0.25}(\text{Si}_7\text{AlO}_{22})(\text{OH})_2$	http://webmineral.com/data/Magnesiohornblende.shtml
Magnesite authigenic			$\text{Mg}(\text{CO}_3)$	http://webmineral.com/data/Magnesite.shtml
Micas	Biotite??		biotite: $\text{KMg}_{2.5}\text{Fe}^{2+}_{0.5}\text{AlSi}_3\text{O}_{10}(\text{OH})_{1.75}\text{F}_{0.25}$	http://webmineral.com/data/Biotite.shtml
Nepheline			$\text{Na}_{0.75}\text{K}_{0.25}\text{Al}(\text{SiO}_4)$	http://webmineral.com/data/Nepheline.shtml
Olivine		Hay (1976)	$\text{Mg}_{1.6}\text{Fe}^{2+}_{0.4}(\text{SiO}_4)$	http://webmineral.com/data/Olivine.shtml
Quartz			(SiO_2)	http://webmineral.com/data/Quartz.shtml
chert				
coesite				http://webmineral.com/data/Coesite.shtml
glass				
glass- altered	Inclgd. palagonite	Hay (1976)		
opaline			$\text{SiO}_2 \cdot 1.5(\text{H}_2\text{O})$	http://webmineral.com/data/Opal.shtml
Pyrite authigenic	Pyritic clays	Hay (1976)	Fe^{2+}S_2	http://webmineral.com/data/Pyrite.shtml
Continued				

Trona	Molds W. Bed II tuffs		$\text{Na}_3(\text{HCO}_3)(\text{CO}_3)\cdot 2(\text{H}_2\text{O})$	http://webmineral.com/data/Trona.shtml
Zeolites			$(\text{Na}_2, \text{K}_2, \text{Ca})_2[\text{Al}_4\text{Si}_{14}\text{O}_{36}]\cdot 15(\text{H}_2\text{O})$	
analcime		Hay & Kyser (2001)	$\text{NaAl}(\text{Si}_2\text{O}_6)\cdot (\text{H}_2\text{O})$	http://en.wikipedia.org/wiki/Analcime http://webmineral.com/data/Analcime.shtml
chabazite		Hay (1976)	$(\text{Ca}, \text{Na}_2, \text{K}_2, \text{Mg})\text{Al}_2\text{Si}_4\text{O}_{12}\cdot 6\text{H}_2\text{O}$ $\text{Ca}_{1.86}\text{Na}_{0.03}\text{K}_{0.2}\text{Mg}_{0.02}\text{Sr}_{0.03}\text{Al}_{3.94}\text{Si}_{8.03}\text{O}_{24}\cdot 13.16(\text{H}_2\text{O})$	http://en.wikipedia.org/wiki/Chabazite http://webmineral.com/data/Chabazite-Ca.shtml#.UxPZgF6torA
erionite			$(\text{Ca}, \text{Na}_2, \text{K}_2)_3\text{Al}_6\text{Si}_{10}\text{O}_{32}\cdot 12\text{H}_2\text{O}$ $(\text{Na}_2, \text{K}_2, \text{Ca})_2[\text{Al}_4\text{Si}_{14}\text{O}_{36}]\cdot 15(\text{H}_2\text{O})$	http://webmineral.com/data/Erionite-Na.shtml#.UxPb1V6torA
phillipsite			$(\text{Na}_2, \text{K}_2, \text{Ca})_2\text{Al}_4\text{Si}_{14}\text{O}_{36}\cdot 15\text{H}_2\text{O}$ $\text{K}_{0.8}\text{Na}_{0.7}\text{Ca}_{0.7}\text{Si}_{5.2}\text{Al}_{2.8}\text{O}_{16}\cdot 6(\text{H}_2\text{O})$	http://en.wikipedia.org/wiki/Phillipsite http://webmineral.com/data/Phillipsite-K.shtml#.UxPa4l6torA

Sources are as cited, or from multiple sources.

Appendix C Age Model Development

Appendix C.1 Age Model: Summarized Results

Sample Number	Jarr-Deino Age, Ma	"Depth" from Bottom, m	Notes
153-IF	1.803	27.40	Three points held out, as redundant, to prevent curve kinks
53-IE	1.831	24.28	
54-IE	1.831	24.24	
-----	-----	-----	-----
151-IF bottom	1.803	27.15	Oldest of Tuff IFs
52-IE	1.831	24.53	
57 IE Vitric	1.835	24.00	
61 ID?	1.839	23.40	
64 IC?	1.843	22.71	
67 IB	1.848	21.87	
145	1.857	19.60	
104	1.869	16.70	
100	1.871	16.05	
97	1.872	15.82	
95	1.873	15.56	
92	1.875	15.09	
85	1.878	14.20	
128	1.890	11.40	
126	1.891	11.11	
124	1.893	10.74	
117	1.898	9.45	
24	1.916	4.95	
19 IA top	1.920	3.87	Youngest of Tuff IAs
-----	-----	-----	-----
18 IA	1.920	3.60	Three held out as redundant, to prevent curve kinks
17 IA	1.920	3.40	
16 IA	1.920	3.20	

Appendix C.2 Basic Stratichronology Ages

Basic Set						
Modified by Deino 2012						
Tuff IA	1.918		Deino (2012)	Hay & Kyser (2001): 1.92 falls in error range		
IA to IB sed	22 cm/ky	Non-tuff lithology	Deino (2012)	Hay & Kyser (2001): 17 cm/ky		
Tuff IB	1.848	"±-0.003	Deino (2012)		IB-IF, 12 cm/ky	Holdship (1976)
IB to IE sed	11 cm/ky		Deino (2012)			
Tuff IC			Deino (2012)			
Tuff ID	1.839	"±-0.011	Deino (2012) interpolation using sed rate 11 cm/ky			
Tuff IE	1.831	"±-0.004	Deino (2012)			
IE to IF sed	9 cm/ky	Non-tuff lithology	Deino (2012)	Hay & Kyser (2001): 12 cm/ky		
Tuff IF	1.803	"±-0.002	Deino (2012)			
Stratigraphic Column (Ashley et al., 1999)						
Tuffs below seem to fit the right sequence, but there are a few other sampled tuffs missing name IDs, and some identifying notes on the stratigraphic column are vague.						
IA		L-16, L-17, L-18, and L-19			All contiguous	
IB		L-67				
IC ??		L-64				
ID		L-61				
IE		L-57, L-54, L-53, and L-52		L-57 and L-54 separated by non-tuff L-56 and 55		
IF		L-151 and L-152				
BED II Lower discontinuity		Top of L-169				

Appendix C.3 Deposit Age Reconciliation Computations: Including Checks, Iterations, Age Determinations, and Interpolations for Model Construction

	Deposit top cm	Deposit bottom cm	Sediment Thickness cm	Deino sed. rates cm/ky		GA-L-x-99	TUFF or SED.	Deino Ages (2012 and 2013)	Computed Age		
L-2 @ 25 cm to IA bottom @	306		281	23.7	11.9	2	Extrapolating before		1.932		
L-4 @ 75 cm to IA bottom @	306		231	23.7	9.7	4	Tuff IA Weak assumption		1.930		
L-10 @ 200 cm to bottom IA	306		106	23.7	4.5	10			1.924		
	383	306				16to19	IA	Consensus value= 1.920	1.920	1.924 Hay & Kyser (2001) sed.	
	2188	383	1805				Top IA to Bottom IB Sediment	not 1.918		Extrapolation	
			-11	23.7		24					
		List of -->> tuffs to be	-10	23.7		25					
		subtracted (-)	-2	23.7		113to114					
			-2	23.7		114to115					
	926		-2	23.7		117					
	1074	400	-3	23.7	27.3	124	Strat column says 1074 cm		1.893	OR 1.893	All pretty close, so
	1111	400	-1	23.7	28.7	126	Strat column says 1111 cm		1.891	1.891	stay with original
	1140	400	-4	23.7	29.9	128	Strat column says 1140 cm		1.890	1.890	EXCEL depth-data list
	1420	400	-2	23.7	41.6	85			1.878	1.878	"
	1509	400	-2	23.7	45.2	92	Strat column says 1509 cm	Curve bend 1.869 -1.878 see mismatch	1.875	1.875	"
	1556	400	-6	23.7	47.1	95	Strat column says 1556 cm	Ashley printed sheet & Strat measures	1.873	1.873	"
	1582	400	-2	23.7	48.0	97	Strat column says 1582 cm		1.872	1.872	"
	1605	400	-4	23.7	48.9	100	Strat column says 1605 cm		1.871	1.871	"
			-12	23.7		104					
			-2	23.7		138					
			-11	23.7		145		Included trivial tuffs.			
Continued											

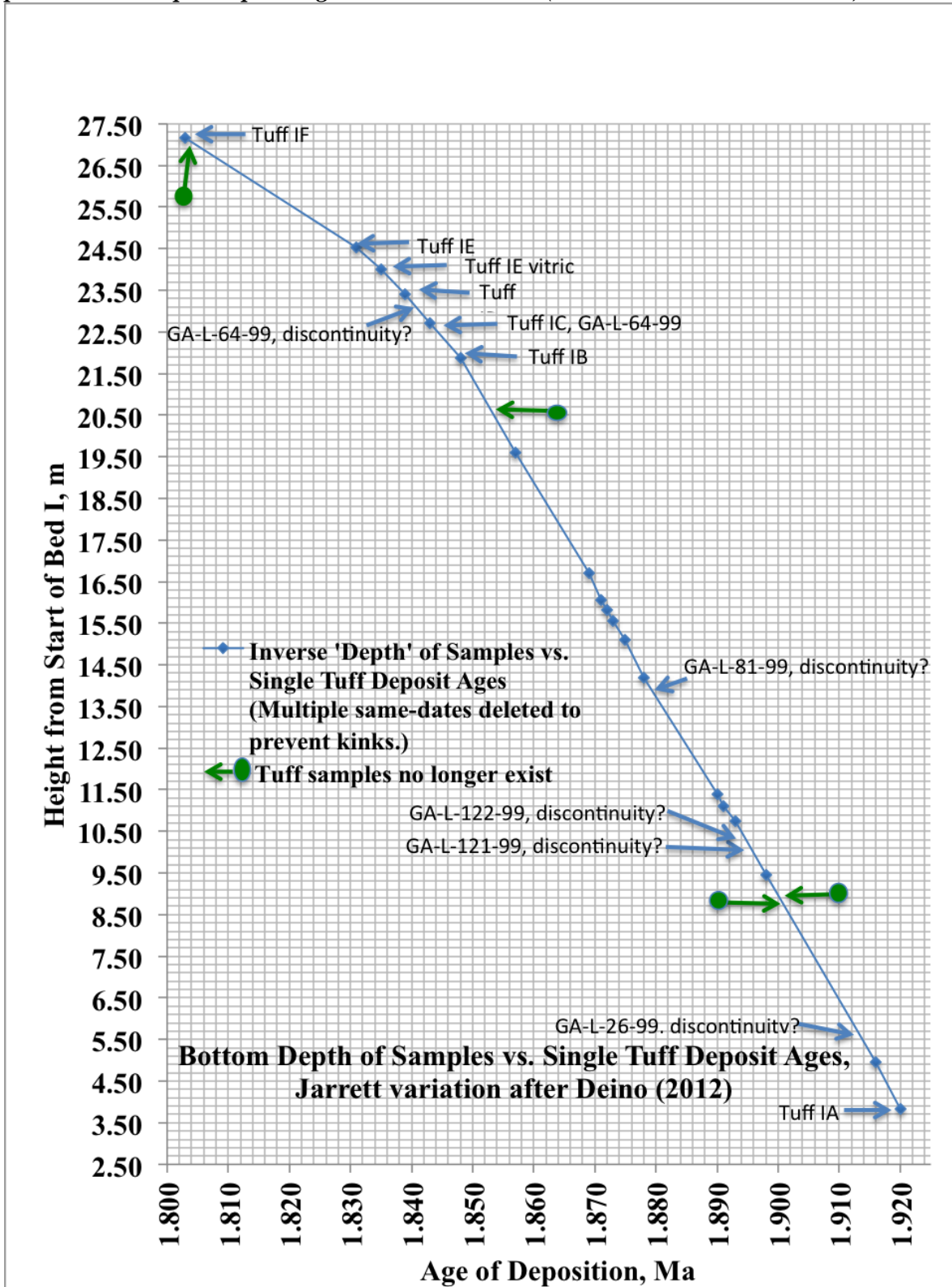
	Deposit top cm	Deposit bottom cm	Sediment Thickness cm	Deino sed. rates cm/ky		GA-L-x-99	TUFF or SED.	Deino Ages (2012 and 2013)	Computed		
					ky				Age		
			-21	23.7		150		To get best fit in 72 ky,			
		Total Sediment	1708	23	74	23 tried per Deino (17Jul13)		74 vs. 72 ky excell, BUT use <u>1708/72 = 23.7</u>			
								<u>because it really fits</u>			
			(+) = non- tuff to be added								
L-20 @ to 400 top IA	400	387	13	23.7	0.5	20			1.919		
L-24 bott to 400 top IA	494	400	94	23.7	4.0	24			1.916		
113-114 Unnamed bott to	881	400	481			No-name					
400 top IA less other tuffs			-21	23.7	19.4				1.901		
114-115 Unnamed bott to	896	400	496			No-name					
400 top IA less other tuffs			-23	23.7	20.0				1.900		
L-117 bott to top IA	945	400	545			117					
less other tuffs			-25	23.7	21.9	Data list 945 not match strat. column 923			1.898		vs. 1.899 - close
L-86 bott to top IA	1420	400	1020			86					
less other tuffs			-37	23.7	41.5				1.879		
L-87 chert nod bott to	1430	400	1030			87		Curve bend 1.869 -1.878 see mismatch			
top IA less other tuffs			-37	23.7	41.9			Ashley printed sheet & Strat measures	1.878		Chert nodules
Continued											

	Deposit	Deposit	Sediment	Deino		GA-L-x-99	TUFF or SED.	Deino Ages (2012 and 2013)	Computed		
	top	bottom	Thickness	sed.					Age		
	cm	cm	cm	rates	ky						
	cm/ky			cm/ky							
L-104 bott to top IA	1670	400	1270			104					
less other tuffs			-51	23.7	51.4				1.869		
L-138 bott to top IA	1789	400	1389			138					
less other tuffs			-63	23.7	55.9				1.864		
L-145 bott to top IA	1960	400	1560			145					
less other tuffs	Column shows 1960		-65	23.7	63.1				1.857		
	1980 is inside L-146 Typo?										
	2200	2188	-12			67	IB		1.848	1.845+/-0.002 Blumenschine (2003)	
		measured col.	71	11	6.5		Sediment IB to IC		6 ky gives 1.842 vs. 1.848		
	2296	2271	-25			64	IC??	1.848	Use 1.843 instead of 1.848		Need a gap IB-IC
										1.839+/-0.005 Blumenschine (2003)	
		measured col.	44	11	4.0		Sediment IC to ID		1.842 - 4 ky = overlaps 1.839		
							Sediment IB to ID		4 + 6 ky gives 10 ky vs. 9 ky good		
	2358	2340	-18			61	ID ?	1.839	1.839		Problem of
			42	11	3.8		Sediment ID to IE vitric			4 ky vs. 2 ky bad but small	
	2410	2400	-10			57	IE vitric ?	1.837	Use 1.835 Better timeline fit than Deino date		
Continued											

	Deposit top cm	Deposit bottom cm	Sediment Thickness cm	Deino sed. rates cm/ky	ky	GA-L-x-99	TUFF or SED.	Deino Ages (2012 and 2013)	Computed Age		
	2428	2410					Sediment IE vitric to IE		1.837-2=1.835		
		Carbonate	5			none					
		Sed in IE tuffs	9			56					
		Sed in IE tuffs	4			55					
		Checks	18	9	2.0						
	2466	2428				54,53,52	IE	1.831	1.831		
		2428	-10			54	Strat column says 2428 cm	3-phase IE duration 4 ky; reasonable			
		2439	-10			53	Strat column says 2439 cm				
		2453	-15			52	Strat column says 2453 cm				
	2661	2667	6	9	0.7	39	Column has 39 starting at 2661 ending 2667! 1 dm off				
							Sediment IE to 39		1830		
	2466	2680	214	9	23.8	38					
							Sediment IE to 38		1807		
	2466	2700	234	9	26.0	37					
							Sediment IE to 37		1805		
		Total non-tuff	247	9	27.4		IE to IF Sediment		9 factor gives		
	2750	2710				151-153	IF	1.803	1.803	1.79 Hay & Kyser (2001)	
							IB to IF Sedimentation	44 vs. 45 ky excellent cross-check on combined for factors 11 & 9			
	2750	3013	263	9	29.2	169-170	BEDS I-II LOWER DISCONTINUITY	Major Extrapolation	1.774		

The 22 cm/ky does not fit the interval of 1.918 to 1.848 of 70 ky. The factor must be closer to 23.7 cm/ky obtained by cut-and-try calculating between limits 1.920 and 1.848 Ma.

Appendix C.4 Sample Depth - Age Conversion Chart (Data in Table 5 and Table 4)



Appendix D XRD-determined Major Authigenic Minerals in Tuffs IA - IF

Mineral	Formula
Albite	$\text{NaAlSi}_3\text{O}_8$
Analcime	$\text{NaAl}(\text{Si}_2\text{O}_6) \cdot (\text{H}_2\text{O})$
Ankerite	$\text{Ca}(\text{Fe}, \text{Mg}, \text{Mn})(\text{CO}_3)_2$
Anorthite	$(\text{Ca}, \text{Na})\text{Al}_2\text{Si}_2\text{O}_8$
Anorthoclase	$\text{Na}_{0.75}\text{K}_{0.25}\text{AlSi}_3\text{O}_8$
Bloedite	$(\text{MgNa}_2)\text{S}_2\text{O}_8 \cdot 4\text{H}_2\text{O}$
Calcite	CaCO_3
Dolomite	$\text{CaMg}(\text{CO}_3)_2$
Gypsum	CaSO_4
Hydrotalcite	$\text{Mg}_6\text{Al}_2(\text{OH})_{16}[\text{CO}_3] \cdot 4\text{H}_2\text{O}$
Jarosite	$\text{Ca}_3\text{Si}_4\text{O}_5$
Microcline (interm)	KAlSi_3O_8
Orthoclase	KAlSi_3O_8
Phillipsite	$\text{Na}_{0.9}\text{Ca}_{0.5}\text{K}_{0.6}\text{Si}_{5.2}\text{Al}_{2.8}\text{O}_{16} \cdot 6(\text{H}_2\text{O})$
Sanidine	$\text{K}_{0.75}\text{Na}_{0.25}\text{AlSi}_3\text{O}_8$
Sanidine (high)	$\text{K}_{0.75}\text{Na}_{0.25}\text{AlSi}_3\text{O}_8$
sanidine-like	$\text{K}_{0.75}\text{Na}_{0.25}\text{AlSi}_3\text{O}_8$

Appendix E Tuff Deposition History (Figures 7 and 12)

Tuff Age, Ma	Dry Peak Age & Depth		Inflection Age & Depth		Wet Peak Age & Depth	
					1.774	30.14
			1.783	29.00	↑Weak extrapolation	
1.803	1.803	27.14				
1.803			1.817	25.70		
					1.826	24.76
1.831						
1.831						
1.831						
1.835						
			1.838	24.00		
1.839						
	1.840	23.33				
1.843						
			1.845	22.10		
1.848						
					1.854	20.60
1.857						
			1.861	18.70		
	1.867	17.14				
1.869						
1.871			1.871	16.30		
1.872					1.872	15.95
1.873						
1.875						
			1.877	14.60		
1.878						
	1.882	13.33				
			1.886	12.40		
					1.888	11.97
1.890						
1.891						
1.893						
1.898						
			1.902	8.70		
	1.912	5.95				
1.916						
1.920						
			1.920	3.80		
1.920						
1.920						
1.920					↓Weak extrapolation	
					1.927	2.00

Appendix F Variations on Alkali Oxide Ratios vs. Ca/MgO (Figures 13 and 14)

Tuff (Na ₂ O + K ₂ O)% vs. (CaO/MgO) Ratio					Tuff (Na ₂ O + K ₂ O)%/MgO% vs. CaO%/MgO%				
CaO/MgO	Tuffs =< 1.857 Ma	Tuffs => 1.869 Ma	Analcime Tuffs => 1.869 Ma	Sample ID GA-L	Tuff/Non- Tuff Average Depth of Set	CaO/MgO	Tuffs =< 1.857 Ma	Tuffs => 1.869 Ma	Analcime Tuffs => 1.869 Ma
1.93	10.67			153	27.40	1.93	3.88		
1.43	12.37			151	27.15	1.43	6.80		
4.83	9.69			52	24.53	4.83	4.09		
0.92	11.55			53	24.28	0.92	1.38		
1.62	12.97			54	24.24	1.62	13.44		
0.71	10.76			57	24.00	0.71	2.40		
0.44	10.88			61	24.30	0.44	2.13		
0.99	11.04			64	22.71	0.99	1.93		
0.44	12.17			67	21.87	0.44	5.93		
0.42	12.85			145	19.60	0.42	8.42		
3.95		10.79		104	16.70	3.95		3.30	
1.26		9.42		100	16.05	1.26		1.25	
1.28		10.81		97	15.82	1.28		2.18	
2.04		11.39		95	15.56	2.04		3.70	
2.85		9.29		92	15.09	2.85		1.62	
1.91		10.67		85	14.20	1.91		1.93	
2.00		11.07		128	11.40	2.00		2.60	
1.38		12.06		126	11.11	1.38		2.21	
9.14		5.76		124	10.74	9.14		1.19	
1.79		9.32		117	9.45	1.79		1.10	
0.75		7.85		24	4.95	0.75		0.26	
1.71		7.28		19	3.83	1.71		0.66	
0.78			8.42	18	3.60	0.78			0.52
1.33			7.46	17	3.40	1.33			0.62
2.35		6.94		16	3.20	2.35		0.69	

Appendix G All Tuff Oxide Data for TriPlot - 25 Tuffs (Figure 15)

Sample	MgO	Na2O + K2O	CaO
	Proportion in class (%)		
	Class 1	Class 2	Class 3
153	14.7	56.9	28.40
151	10.8	73.7	15.50
52	10.1	41.2	48.70
53	30.3	41.8	27.9
54	6.2	83.7	10.1
57	24.4	58.3	17.3
61	28.0	59.8	12.2
64	25.5	49.3	25.2
67	13.6	80.4	6.0
145	10.2	85.6	4.2
104	12.1	40.0	47.9
100	28.5	35.6	35.9
97	22.4	48.9	28.7
95	14.8	54.9	30.2
92	18.3	29.6	52.1
85	20.7	39.9	39.4
128	17.9	46.4	35.7
126	21.8	48.2	30.0
124	8.8	10.5	80.7
117	25.7	28.2	46.1
24	49.6	13.1	37.4
19	29.6	19.6	50.7
18	43.3	22.7	33.9
17	33.9	21.0	45.1
16	24.7	17.1	58.2

**Appendix H Major Cations in Zeolites and Primary & Secondary Non-Zeolite Minerals
(Figure 16)**

Jarr-Deino Date (Ma)	Phillipsite	Analcime	K	Mg	Ca	Na
Data spreading coding	1 or 1.1	1 or 1+1.1	2 or 2.1	3 or 3.1	3.9-4-4.1	4.9-5-5.1
1.803	1		2		4	5
1.803			2.1			5.1
1.831	1		2		4.1	5
1.831			2		4	
1.831	1.1		2.1		3.9	5.1
1.835	1		2	3	4	5
1.839	1		2		4	5
1.843			2	3		5
1.848	1		2		4	5
1.857	1		2	3	4	5
1.869			2		4.1	5
1.871			2.1		4	5
1.872			2		4.1	
1.873			2.1		4	
1.875				3	4.1	
1.878			2			
1.890			2	3		5
1.891			2.1	3.1		5
1.893					4	
1.898					4	
1.916				3	4	
1.920			2		4.1	
1.920		1		3	4.2	5.1
1.920		1.1		3.1	4	5
1.920					3.9	4.9

Appendix I Tuff Age & Tuff Type vs. CaO/MgO Ratio (Figure 17)

CaO/MgO (Berry (2012))	Non-zeolite	Phillipsite	Analcime
Oxide Ratio	Age, Ma	Age, Ma	Age, Ma
1.93		1.803	
1.43	1.803		
4.83		1.831	
0.92	1.831		
1.62		1.831	
0.71		1.835	
0.44		1.839	
0.99	1.843		
0.44		1.848	
0.42		1.857	
3.95	1.869		
1.26	1.871		
1.28	1.872		
2.04	1.873		
2.85	1.875		
1.91	1.878		
2.00	1.890		
1.38	1.891		
9.14	1.893		
1.79	1.898		
0.75	1.916		
1.71	1.920		
0.78			1.920
1.33			1.920
2.35	1.920		

Appendix J Tuff Age & Tuff Type vs. Al₂O₃/MgO Ratio (Figure 16)

Al₂O₃/MgO (Berry, 2012)	Non-zeolite	Phillipsite	Analcime
Oxide Ratio	Age, Ma	Age, Ma	Age, Ma
5.23		1.803	
8.79	1.803		
5.40		1.831	
1.24	1.831		
18.46		1.831	
3.13		1.835	
2.81		1.839	
2.17	1.843		
7.73		1.848	
10.74		1.857	
4.00	1.869		
1.34	1.871		
2.53	1.872		
4.59	1.873		
1.64	1.875		
2.32	1.878		
2.61	1.890		
2.14	1.891		
0.79	1.893		
1.00	1.898		
0.13	1.916		
0.78	1.920		
0.60			1.920
0.83			1.920
0.94	1.920		

Appendix K. Cation Oxide Statistical Analysis

Appendix K.1 Variable Input Data

Age	SiO ₂	Al ₂ O ₃	MgO	CaO	Na ₂ O	K ₂ O	Na ₂ O +K ₂ O
0	58.15	14.38	2.75	5.32	4.59	6.07	10.67
0	61.08	15.99	1.82	2.60	3.20	9.17	12.37
0	57.49	12.80	2.37	11.45	3.64	6.05	9.69
0	55.59	10.43	8.40	7.72	2.97	8.58	11.55
0	59.32	17.81	0.96	1.57	5.86	7.11	12.97
0	57.03	14.08	4.49	3.19	4.22	6.55	10.76
0	59.41	14.34	5.10	2.23	4.70	6.18	10.88
0	57.15	12.39	5.72	5.64	2.90	8.14	11.04
0	61.67	15.88	2.05	0.91	5.32	6.85	12.17
0	63.52	16.38	1.53	0.63	6.03	6.82	12.85
1	54.68	13.06	3.27	12.90	4.21	6.58	10.79
1	53.05	10.12	7.55	9.52	2.14	7.29	9.42
1	56.89	12.56	4.96	6.34	3.31	7.50	10.81
1	58.33	14.11	3.08	6.27	3.47	7.92	11.39
1	46.25	9.43	5.73	16.35	2.25	7.03	9.29
1	50.08	12.81	5.52	10.55	3.08	7.59	10.67
1	50.33	11.12	4.26	8.52	3.60	7.47	11.07
1	53.56	11.64	5.45	7.49	3.34	8.72	12.06
1	27.68	3.85	4.86	44.40	2.92	2.85	5.76
1	49.39	8.54	8.50	15.22	3.28	6.05	9.32
1	32.55	3.73	29.81	22.48	5.00	2.85	7.85
1	46.57	8.53	10.99	18.82	2.83	4.45	7.28
1	44.97	9.61	16.05	12.57	5.58	2.84	8.42
1	45.55	9.95	12.01	15.99	4.12	3.35	7.46
1	41.61	9.49	10.07	23.70	3.26	3.69	6.94

Appendix K.2 Correlation Contingency Table

	Age	SiO ₂	Al ₂ O ₃	MgO	CaO	Na ₂ O	K ₂ O	Na ₂ O+K ₂ O
Pearson Correlation								
Age	1							
SiO ₂	-.658 p < .001	1 p						
Al ₂ O ₃	-.650 p < .001	.925 p < .001	1					
MgO	.438 p < .02	-.671 p < .001	-.723 p < .001	1				
CaO	.590 p < .001	-.931 p < .001	-.865 p < .001	.433 p < .02	1			
Na ₂ O	-.391 p < .03	.241 N.S	.398 p < .03	.067 N.S	-.351 p < .05	1		
K ₂ O	-.368 p < .04	.751 p < .001	.636 p < .001	-.632 p < .001	-.698 p < .001	-.254 N.S	1	
Na ₂ O+K ₂ O	-.581 p < .001	.873 p < .001	.848 p < .001	-.583 p < .001	-.883 p < .001	.310 N.S	.841 p < .001	1

N.S. = not significant at $p > .05$

Appendix L: XRD Diffraction Scan

Individual scans start on the next sheet.

